Studies by the U.S. Geological Survey in Alaska, Volume 15

Arctic Alaska's Lower Cretaceous (Hauterivian and Barremian) Mudstone Succession—Linking Lithofacies, Texture, and Geochemistry to Marine Processes

Professional Paper 1814–B

U.S. Department of the Interior
U.S. Geological Survey

FRONT COVER

Photograph of a very good outcrop of the Lower Cretaceous mudstone succession at Marsh Creek in the northern area of the Arctic National Wildlife Refuge, Alaska. Prominent, blocky, light-colored intervals of carbonate-cement-dominated mudstone are interbedded with predominant, dark-colored lithofacies consisting of silt- and clay-rich mudstones of the pebble shale unit (U.S. Geological Survey photograph by Margaret A. Keller).

Studies by the U.S. Geological Survey in Alaska, Volume 15

Arctic Alaska's Lower Cretaceous (Hauterivian and Barremian) Mudstone Succession—Linking Lithofacies, Texture, and Geochemistry to Marine Processes

By Margaret A. Keller and Joe H.S. Macquaker

Professional Paper 1814–B

U.S. Department of the Interior
U.S. Geological Survey

U.S. Department of the Interior
SALLY JEWELL, Secretary

U.S. Geological Survey
Suzette M. Kimball, Acting Director

U.S. Geological Survey, Reston, Virginia: 2015

Suggested citation:
Keller, M.A., and Macquaker, J.H.S., 2015, Arctic Alaska's Lower Cretaceous (Hauterivian and Barremian) mudstone succession—Linking lithofacies, texture, and geochemistry to marine processes, *in* Dumoulin, J.A., ed., Studies by the U.S. Geological Survey in Alaska, vol. 15: U.S. Geological Survey Professional Paper 1814–B, 35 p., http://dx.doi.org/10.3133/pp1814B.

ISSN 2330-7102 (online)

Acknowledgments

Many colleagues are appreciated for their contributions to these studies, particularly Gil Mull and Ken Bird for generously sharing their knowledge of the North Slope during many helpful discussions and Paul Lillis for assistance with organic geochemistry. David Houseknecht, Steve Bergman, Kevin Taylor, Kevin Bohacs, Erik Reimnitz, Larry Phillips, Peta Mudie, Albert Holba, Art Grantz, Tom Moore, and Mike McCormick provided helpful discussions and (or) reviews of our earlier work. This manuscript benefited tremendously from the comments/suggestions of reviewers Larry Phillips and Ken Bird, volume editors Julie Dumoulin and Cynthia Dusel-Bacon, and text editor Jim Hendley. Thanks go to the U.S. Geological Survey and the University of Manchester for funding this research, Mobil Oil Company (and now Exxon/Mobil) for permission to sample and analyze their core, Michael Mickey and Hideyo Haga for sharing their analysis of the fauna and flora, Mary McGann and Isabella Premoli Silva for identifying calcitic, benthic foraminifera in thin section, and Zenon Valin for graphics advice and assistance.

Contents

Figures

Table

Studies by the U.S. Geological Survey in Alaska, volume 15
Edited by Julie A. Dumoulin
U.S. Geological Survey Professional Paper 1814–B
[Also see http://pubs.usgs.gov/AK_studies/]

Arctic Alaska's Lower Cretaceous (Hauterivian and Barremian) Mudstone Succession—Linking Lithofacies, Texture, and Geochemistry to Marine Processes

By Margaret A. Keller[1] and Joe H.S. Macquaker[2]

Abstract

We present new images and descriptions of the lithofacies and organic facies of the pebble shale unit and lower part of the Hue Shale (Lower Cretaceous) of Arctic Alaska at a high magnification that illustrates their textural characteristics. Our aims were to describe and determine the distribution of facies in these petroleum source rocks and to identify the processes that formed them. We sampled at high-resolution and applied new petrographic techniques combined with scanning electron microscopy and geochemical analyses to samples collected from three widely spaced sections—located in exposures along the Canning River and continuous core from the Mikkelsen Bay State 1 and Orion 1 wells.

Results from these three locations indicate that this succession consists primarily of clay-rich mudstones that are variously silt- or sand-bearing and clay-dominated mudstones that exhibit mainly relict, 2–5 millimeter thick bedding and common but variable microbioturbation, rare macrobioturbation, and common fabrics of pelleted clay and silt. These mudstones contain rare, poorly sorted, silt-rich basal laminae that are often discontinuous and have wavy, sharp bases and crude upward fining. In addition, mud-supported, outsized clasts (dropstones) of fine sand to pebble size are present throughout the succession as isolated clasts or in clusters. We interpret these textures and much of this succession to result from intermittent deposition by suspension settling from melting seasonal sea ice—sometimes sediment-laden—and associated primary productivity. Overall, this mudstone succession fines and deepens upward from the pebble shale unit into the Hue Shale. In the Hue Shale of the Orion well, however, different processes intermittently deposited thin, discrete intervals of coarser sediment that probably represent deposition from density currents. Also in the Hue Shale of the Orion well, several thicker sandstone and silt-dominated mudstone units with discordant, scoured bases and cut and fill structures represent erosion during higher energy events such as major storms.

Other lithofacies within the succession are graded tuffs/bentonites and tuffaceous/bentonitic mudstones from episodic volcanic ash falls; these are abundant in the Hue Shale, and very rare in the pebble shale unit of the two wells. Organic-carbon rich strata associated with volcanic ash intervals of the pebble shale unit and Hue Shale in the Mikkelsen 1 well have some of the best petroleum source rock potential determined for this succession. Authigenic pyrite and carbonate-cement-dominated mudstone are also present in both units of all three sections. The carbonate-cemented units indicate breaks in sedimentation and are common in the Hue Shale and in sections of the pebble shale unit interpreted to be more distal, such as along the Canning River.

Our results document the variation in facies and textures of the Hauterivian and Barremian Lower Cretaceous mudstone succession of Arctic Alaska. Comparison of these characteristics to the products of modern processes on the North Slope of Alaska, in the Beaufort Sea, and elsewhere suggest that this succession formed primarily from depositional processes related to seasonal sea ice with intermittent fluvial-sourced sediment deposited by density currents and episodic erosion and reworking by storms and other currents.

Introduction

The North Slope of Alaska extending into the Beaufort Sea is an important petroleum province with multiple mudstone/shale formations of Mesozoic to Cenozoic age (fig. 1). These strata contain organic carbon-rich intervals that are the source rocks for petroleum accumulations in this region (for example, Magoon and others, 1987; Magoon and others, 1999; Keller and others, 1999; Bird, 2001; Bird and Houseknecht, 2005; Peters and others, 2006) and clay-rich intervals that provide seals for petroleum accumulations (Bird, 2001).

Before the past two decades, the lithofacies of the dark gray to black fine-grained, organic carbon-rich siliciclastic sedimentary rocks of the North Slope had primarily been described from observations at hand specimen and outcrop scale and generally identified as various types of shale. For example, lithofacies descriptions of the Lower Cretaceous siliciclastic succession (fig. 2) include (1) black laminated shales with high organic content; (2) dark gray to black shales; (3) fissile, black organic-rich shales (for example, Molenaar and others, 1987; Molenaar, 1988; Mull, 1987);

[1]U.S. Geological Survey.

[2]Memorial University of Newfoundland, St. John's, Canada.

and (4) black anaerobic-dysaerobic shales and silty aerobic shales (Blanchard and Tailleur, 1983). The terms paper shale, carbonaceous shale, and euxinic shale have also been used for specific lithofacies (for example, Blanchard and Tailleur, 1983; Mickey and others, 2006).

During the 1990s, many new studies of mudstones and shales demonstrated that important variation in composition and texture had not been recognized previously in studies at hand-specimen and outcrop scales. The application of new petrographic techniques in addition to geochemical and other methods to describing shales and mudstones in "classic" and much-studied fine-grained rock successions worldwide resulted in many new discoveries (for example, Macquaker and Gawthorpe, 1993; Macquaker, 1994; Macquaker and others, 1998; Macquaker and Taylor, 1996; Kemp, 1996; O'Brien; 1996; Pike and Kemp, 1996; Schieber, 1994a,b; 1999). These investigations especially indicated the need for finer scale observations of mineralogic components, sedimentary structures, textures, and depositional fabrics, not only to interpret the depositional and diagenetic processes that formed them, but also to understand the temporal and spatial distribution of the resulting facies. At the same time, a new assessment of the petroleum potential of the 1002 area of the Arctic National Wildlife Refuge (ANWR) by the U.S. Geological Survey (USGS) (Bird, 1999; Keller and others, 1999) called for a better understanding of the petroleum source rocks in this part of Alaska.

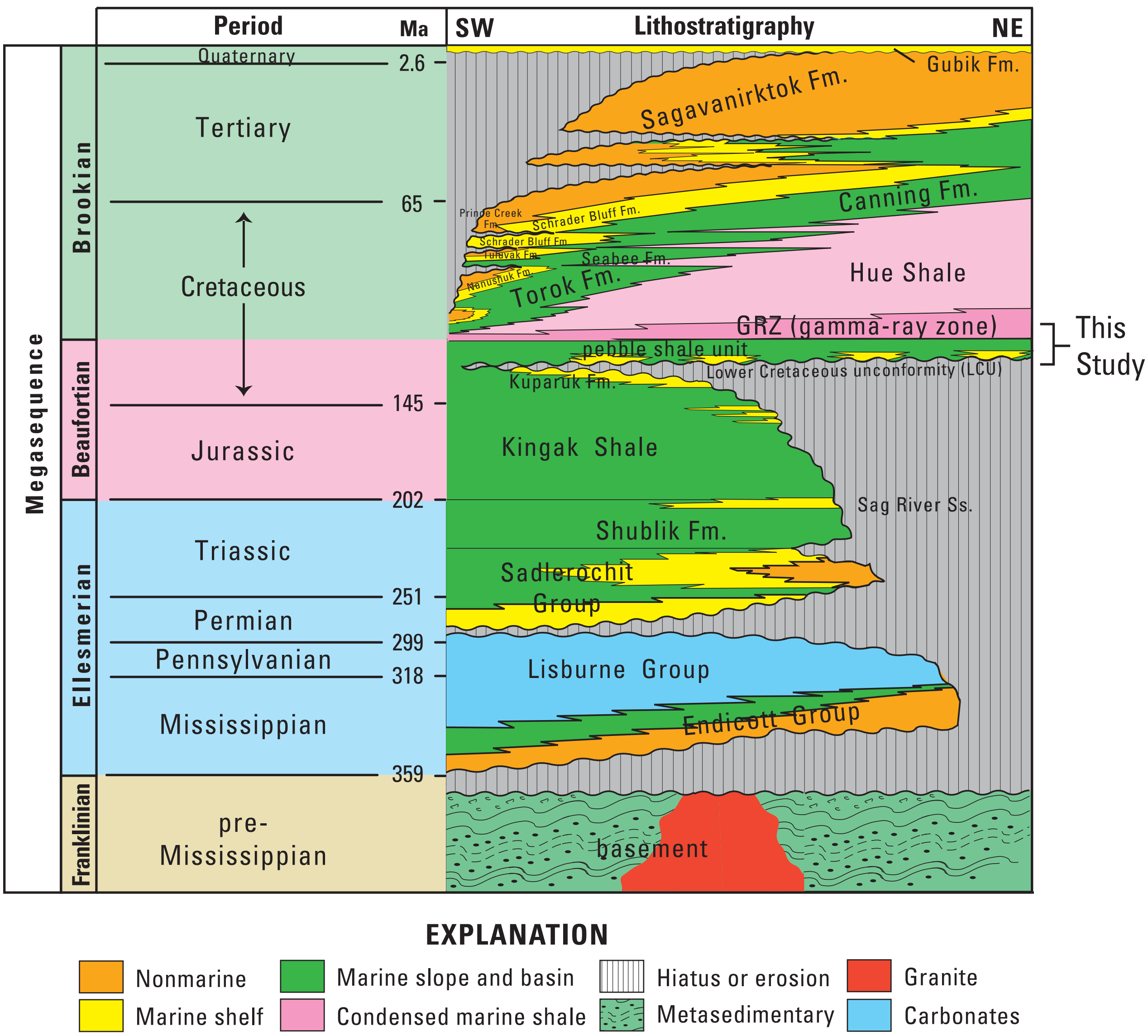

Figure 1. Diagram showing simplified stratigraphy of the central North Slope, Alaska (slightly modified from Kenneth J. Bird, U.S. Geological Survey, written commun., 2010; absolute ages from Walker and Geissman, 2009). Wavy and horizontal to subhorizontal rock unit contacts are unconformities. Jagged and tapering contacts show interfingering rock units. Ma, mega-annum; Fm., formation; Ss. Sandstone; SW, southwest; NE, northeast.

Figure 2. Photograph of the Lower Cretaceous mudstone succession at Marsh Creek, Alaska, showing prominent and more resistant, light-colored intervals of carbonate-cement-dominated mudstone (concretionary carbonate) interbedded with dark intervals of silt- and clay-rich mudstones of the pebble shale unit (U.S. Geological Survey photograph by Margaret A. Keller).

Alaska Studies

The factors described above set the stage for initiating our studies of the Lower Cretaceous mudstone succession on the North Slope, Alaska, beginning at exposures along the Canning River in 1997 (Macquaker and others, 1999) and subsequently with core from the Mikkelsen Bay State 1 well in 2000 (Keller and Macquaker, 2001; Keller and others, 2001; Macquaker and Keller, 2005) and the Orion 1 well in 2002 (Keller, 2006; Keller and others, 2009) (fig. 3). The objectives of these investigations were to describe and understand the origin of facies types and characteristics—including constituent components, mineralogy, textural variation, and temporal distribution; depositional settings and processes; and petroleum-source-rock potential. This predominantly mudstone succession represents an important time of tectonic transition from the final stage of rifting (subsidence of rift shoulder), represented by northern or locally derived sediment of the Kemik Sandstone and pebble shale unit, to postrifting distal facies of orogenic (ancestral Brooks Range) derived sediment of the Hue Shale (figs. 1, and 4) (Bird and Molenaar, 1987; Molenaar, 1988). The studied succession is the Lower Cretaceous pebble shale unit of Hauterivian-Barremian age (Mull, 1987; Bird and Molenaar, 1987; Molenaar and others, 1987; Mickey and others, 2006) and the contiguous lower part of the Hue Shale (also defined as the gamma-ray zone or GRZ) of Barremian to possibly early Albian age (Michael B. Mickey, Micropaleo Consultants, Inc., written commun., 2000; Mickey and others, 2006).

Prior investigations of measured sections, plus outcrop and well-sample descriptions, have shown that the pebble shale unit and the Hue Shale are both primarily shale/mudstone; however, different organic facies as determined by Rock-Eval pyrolysis and maceral identification have been observed in these formations (for example, Magoon and others, 1987, p.139–143). Both shale/mudstone units also contain other lithofacies (for example, Blanchard and Tailleur, 1983; Mull, 1987; Bird and Molenaar, 1987) such as ash-fall tuffs, which are abundant in the Hue Shale but rare in the pebble shale unit. In addition, Bird and Molenaar (1987) note that ironstone concretions are common in the pebble shale unit of the ANWR. However, the spatial and temporal variability of these organic facies and lithofacies/lithologies have not been determined basinwide, nor have they been linked to age and environmental data determined from micropaleontological studies. Neritic, bathyal, and distal (starved basin) environments have been interpreted for different parts of these mudstone successions based on microfossil assemblages (for example, Mickey and Haga as cited in Mull, 1987; Mickey and others, 2006) and studies using both paleontology and seismic data (for example, fig. 4 of Molenaar, 1988).

Before our studies, no systematic high-resolution lithofacies analysis of these fine-grained rocks using optical and electron optical petrography (scanning electron microscopy, SEM) had been done, and therefore, the different lithofacies and sedimentary fabrics (representing evidence of the processes forming them) had not been distinguished. Furthermore, prior data collected from the organic facies were not linked to lithofacies or sedimentary processes interpreted from textural evidence. In addition, the likelihood of a cold climate due to the high latitude setting—implying the possibility of a seasonally cold winter—was not generally considered for this succession, except by Kemper (1987), Mull (1987), and Frakes and Francis (1988). This may have been because of the warmer climate and ocean hypothesized for the mid-Cretaceous (for example, Huber, 1998) and because many studies of modern Arctic sediment and sedimentary processes relevant as an analog to these Lower Cretaceous rocks were in their infancy (for example, Barnes and others, 1982; Kempema and others, 1989; Reimnitz and others, 1993, 1998). Similarly, modern studies of deep-sea cores, sedimentary environments, and processes in other regions have contributed immensely to understanding ancient fine-grained sedimentary rocks (for example, Honjo and Roman, 1978; Kranck, 1984; Alldredge and Silver, 1988; Domack, 1988; Kranck and Milligan, 1991; Alldredge and others, 1993; Eyles, 1993; Bromley, 1996; Gorsline and others, 1996; Kranck and others, 1996a,b; Pike and Kemp, 1996; Lowe and Guy, 2000; McCave and others, 2001; Lisitzin, 2002).

In this report, we review the results and conclusions from our prior high-resolution studies of the Lower Cretaceous succession at two localities on the North Slope and present new results from a third section located in the adjacent Beaufort Sea (fig. 3). We address three basic questions:

1. What lithofacies and organic facies are present in the Lower Cretaceous succession at each of these locations on the North Slope? And how do these vary over time?
2. What kinds of primary and secondary sedimentary textures, structures, and fabrics are present?
3. What do these characteristics indicate about the origin and distribution of these rocks?

Our earlier studies focused primarily on the pebble shale unit in outcrop on the Canning River (Macquaker and others, 1999), also known as the Emerald Island Section (Bergman and others, 1995), and the pebble shale unit plus the lowermost part of the Hue Shale in the Mikkelsen Bay State 1

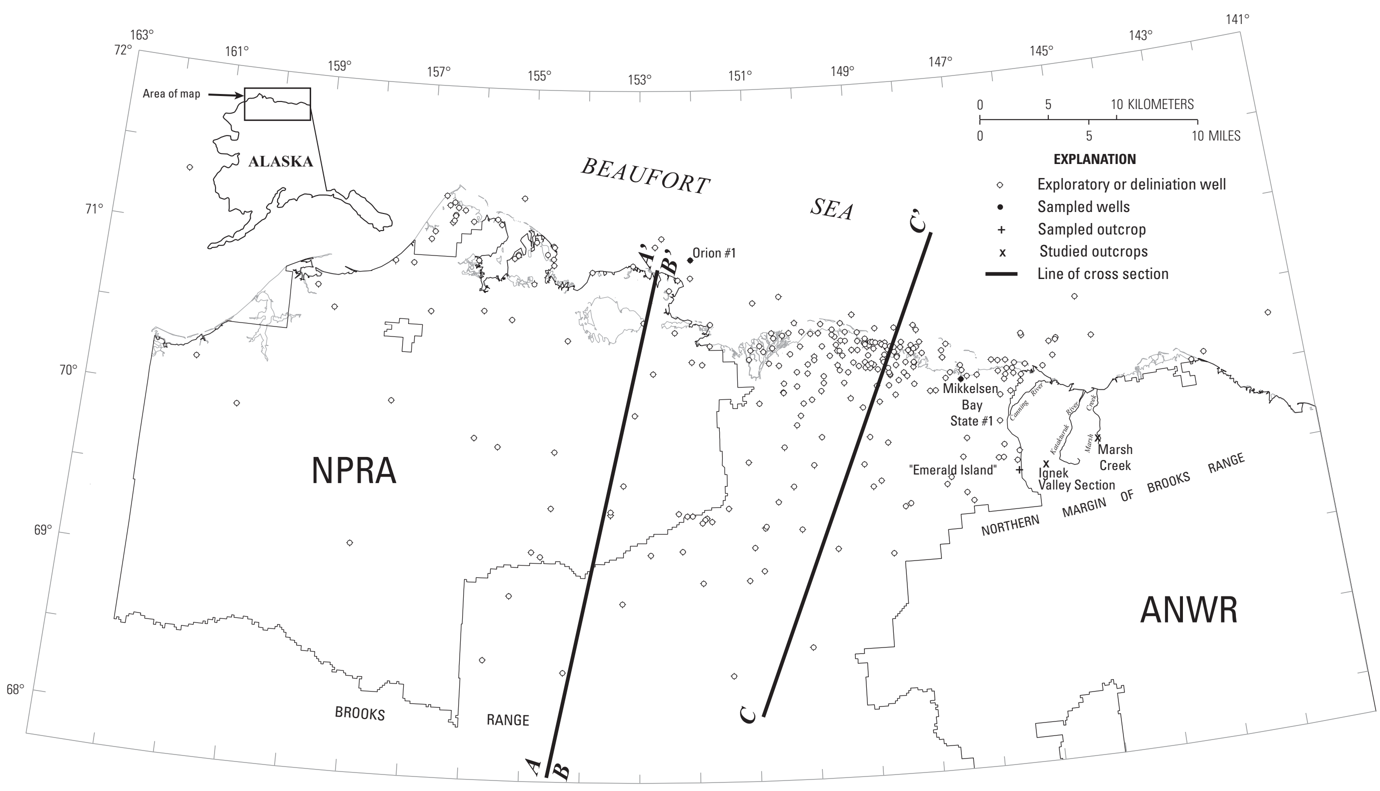

Figure 3. Index map of the central North Slope, Alaska, showing the locations of studied and sampled sections in outcrop and wells and of schematic cross sections shown in figure 4. Also shown are the locations of the National Petroleum Reserve in Alaska (NPRA), the Arctic National Wildlife Refuge (ANWR), and the type section of the Hue Shale in Ignek Valley. Map slightly modified from Kenneth J. Bird, U.S. Geological Survey, written commun., 2010.

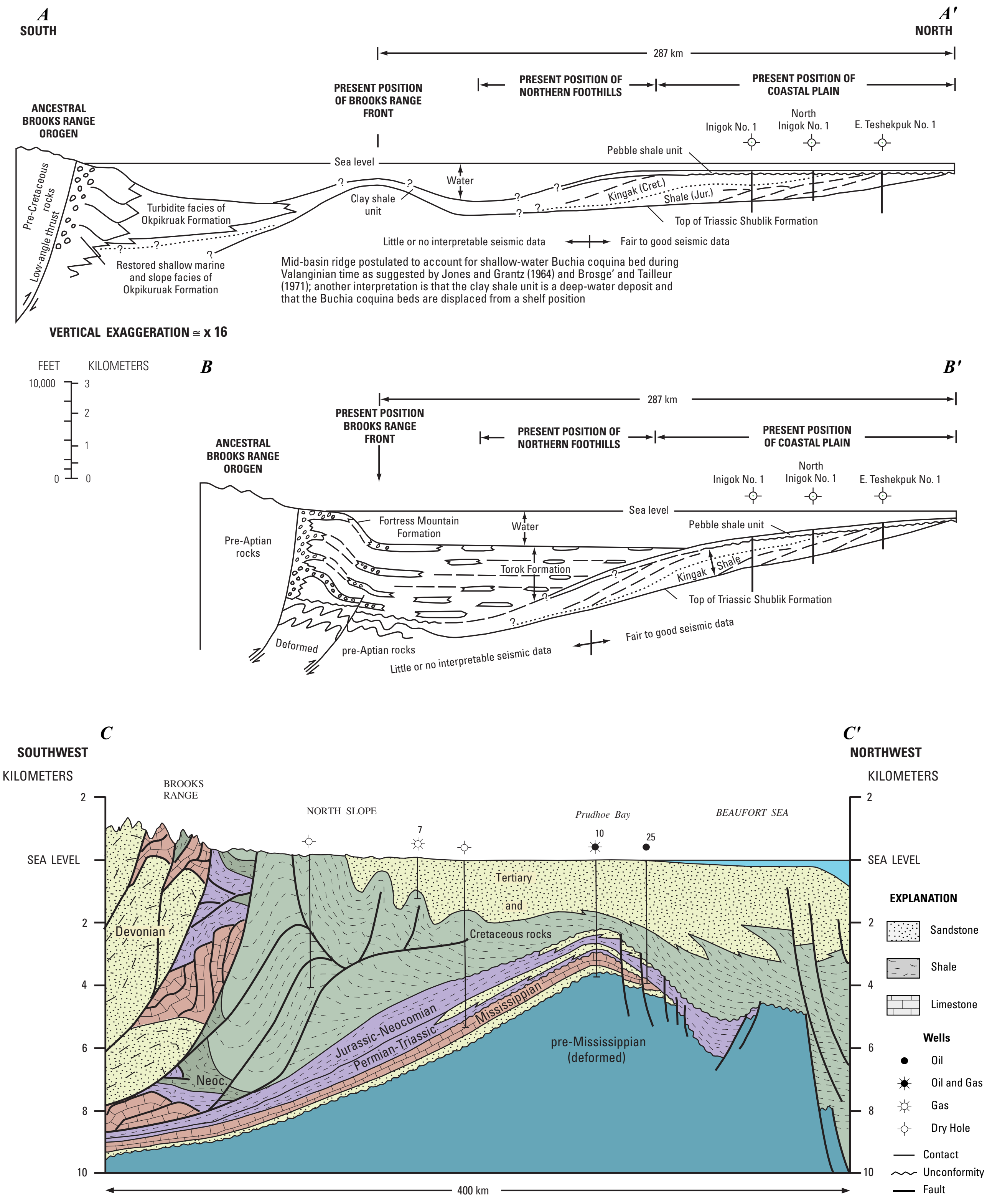

Figure 4. Diagram of restored cross sections across the Colville Basin, North Slope, Alaska, showing Lower Cretaceous rocks at three different times in the Cretaceous (sections *A* and *B* from Molenaar, 1988; section *C* modified slightly from Bird and Bader, 1987). See figure 3 for locations. All sections have the same vertical exaggeration. *A-A′*, Restored cross section at the end of pebble shale (Neocomian) time (from Molenaar, 1988). *B-B′*, Restored cross section at the end of Fortress Mountain-lower Torok (early Albian) time (from Molenaar, 1988). Note that the upper part of the pebble shale unit shown in sections *A* and *B* includes the gamma-ray zone (GRZ) of the Hue Shale. *C-C′*, Present-day schematic stratigraphic relations through several oil and gas fields—North Star oil field (25), Prudhoe Bay and Kuparuk River oil fields (10), and Gubik gas field (7) (modified slightly from Bird and Bader, 1987). Cret., Cretaceous; Jur., Jurassic; km, kilometers.

well (Keller and Macquaker, 2001; Keller and others, 2001; Macquaker and Keller, 2005). Our new results are from the completely cored, lower part of the Lower Cretaceous section in the Orion 1 well of the Beaufort Sea approximately 140 miles northwest of the Mikkelsen 1 well (fig. 3). In the Orion 1 well our samples cover the complete pebble shale unit and extend higher into the GRZ through more section than in the Mikkelsen 1 well.

We emphasize that distinguishing the transport and depositional processes of some of the fine-grained lithofacies of these successions is equivocal and that our study is a work in progress. It is important to note that, for the most part, the sedimentary fabrics and textures of these mudstone lithofacies are only evident at microscopic scale—and at a minimum scale, from enlarged scans of thin sections. This requires excellent quality, extra thin (20 micrometers, µm) thin sections. Because this was technically challenging until recently, and not commonly done, proportionately fewer published examples of lithofacies and sedimentary fabrics of mudstones exist—both from ancient lithified sediments and modern sediment—as compared to sandstones and coarser sedimentary rocks.

Geologic Background

Study of the Cretaceous and lower Tertiary succession on the North Slope, Alaska, is challenging due to "discontinuous outcrops, structural complications, and a thick shale succession" which makes "physical tracing of units difficult or impossible over much of the area" (Molenaar, 1983, p. 1066). Pervasive permafrost has also physically weathered the outcrops so that apparently well-lithified samples break apart into small pieces. Originally described by Collins and Robinson (1967) in the subsurface near Barrow, the pebble shale unit is widely recognized in drill core from the North Slope even though it is not well exposed at the surface (Mull, 1987). Because of these factors, most prior study has been on well samples (for example, Carman and Hardwick, 1983) and a few good outcrop sections in Ignek Valley at Hue Creek (for example, Molenaar and others, 1987; Magoon and others, 1987), at Marsh Creek (Mull, 1987), and along the Canning River at Emerald Island (fig. 3) (Bergman and others, 1995; Macquaker and others, 1999).

From Molenaar's (1988) regional study of the tectonic evolution of the North Slope of Alaska, we infer that during the Early Cretaceous the three mudstone sections of this report were deposited at distances of many miles from each other (figs. 3 and 4), and very likely in different depositional environments and paleodepths. The sections also differ in their proximity to the proposed northern source area during pebble shale unit deposition as well as to their proposed southern, Brooks Range source area during deposition of the Hue Shale (fig. 4). In Molenaar's model for the deposition of the Lower Cretaceous succession, based primarily on seismic data (fig. 4*A* and *B*), south dipping clinoform sequences of the Kingak Shale (Jurassic and Early Cretaceous age) are truncated by a regional Lower Cretaceous unconformity (LCU) that is overlain in places by the discontinuous Kemik Sandstone followed by the pebble shale unit—generally 200–400 feet (ft) thick where present.

Molenaar (1988) considered the pebble shale unit to be derived both locally and from the same northern source area as the Kingak Shale and Kemik Sandstone. Its deposition followed the rapid transgression that resulted in deposition of the Kemik Sandstone (fig. 4A; Molenaar, 1988). Mull (1987, p. 412) emphasizes that even though the pebble shale unit and the Kemik Sandstone are both dated as Hauterivian-Barremian, "each Kemik facies is overlain at a sharp contact by the pebble shale unit without evidence of interfingering with the underlying strata, . . . suggesting rapid marine transgression in which the pebble shale unit represents an effective time line"—at least locally.

From a study of the depositional environments of the "pebble shale" in the National Petroleum Reserve–Alaska (NPRA) using clay mineralogy, organic geochemistry, micropaleontology, and sedimentary structures from core and cuttings, Blanchard and Tailleur (1983, p. 424) described the pebble shale in NPRA (which included the gamma-ray zone at that time) as consisting of "black anaerobic-dysaerobic shales, silty aerobic shales, pebbly mudstones, and sandstones." They interpreted their results as indicating "a stratigraphic sequence through the Neocomian of upper to lower slope facies followed by inner and outer shelf facies and finally deposition of euxunic [sic] sediments."

Deposition of the pebble shale unit was followed by deposition of the Hue Shale—a fine-grained succession from a genetically different depositional system sourced from the ancestral Brooks Range to the south and deposited on the north side of the Colville Basin, on the Barrow Arch, and probably on the area north of the arch. The Hue Shale (approximately 1, 000 ft (300 meters, m) or less in thickness) is an eastward thickening succession that includes "distal condensed shale facies" (Bird and Molenaar, 1987, p. 51).

Existing paleontologic age data have some uncertainty regarding which parts of the Hauterivian (approximately 134–131 million years), Barremian (approximately 131–126 million years), and Aptian (approximately 126–113 million years) to early Albian (approximately 113-? million years) stages are present in the three Lower Cretaceous sections of this study (Walker and Geissman, 2009). Mickey (Michael B. Mickey, oral commun., 2000) indicated that the lower part of the pebble shale unit at the Canning River section was in part Hauterivian Stage; however, subsequent results by Mickey (in van der Kolk, 2010) indicate a Barremian age. The pebble shale unit in the Mikkelsen 1 well is possible Hauterivian Stage in the lower part and above that probable Barremian to early Albian stages (Michael B. Mickey, written commun., 2000). The pebble shale unit in the Orion 1 well is also part Hauterivian Stage and part Barremian Stage—zone F-12 (Mickey and others, 2006). The Hue Shale is probable Barremian to early Albian stages in the Mikkelsen well (Michael B. Mickey, written commun., 2000) and Barremian to early

Albian stages (zones F-12 and Pm18a) in the Orion well (Mickey and others, 2006).

A widespread unconformity on the North Slope that formed during the Early Cretaceous "progressively truncates all older units northward onto the Barrow arch" (Bird, 2001, p. 140), but does not extend as far south as the Emerald Island section of the Canning River where the pebble shale unit rests conformably on the Lower Cretaceous, Hauterivian-Barremian Kemik Sandstone, which in turn conformably overlies the Hauterivian upper part of the Kingak Shale (Macquaker and others, 1999). In the Mikkelsen Bay State 1 well, the Lower Cretaceous unconformity rests on limestone of Mississippian age. Here the pebble shale unit, of possible Hauterivian age in the lower 18 ft (Michael B. Mickey, written commun., 2000), was deposited conformably on a section of fine-grained sandstone that overlies Mississippian limestone. This approximately 90-ft thick section of sandstone, here considered the Kemik Sandstone, is of possible Hauterivian age in the upper part (Michael B. Mickey, written commun., 2000). In the Orion 1 well the pebble shale unit, in part of Hauterivian Stage zone F13a age (Mickey and others, 2006), unconformably overlies pre-Mississippian argillite basement rocks.

Methods, Terminology, and Stratigraphy of Samples

We photographed and described each mudstone section to characterize the overall facies variability. We then collected hand specimens to make thin sections for describing the lithofacies in greater detail and for geochemical analyses. At the Canning River section, we collected 39 samples over 13 m (42.6 ft) from the section interpreted as the lower part of the pebble shale unit at 30–50 centimeters (cm) (11.8–19.7 inches) intervals or at visible changes in facies (Macquaker and others, 1999) (fig. 5). Similarly, in the Mikkelsen Bay State 1 well (hereafter referred to as the Mikkelsen 1 well), we collected 49 samples from 101 ft (30.8 m; original measurements in feet) of section interpreted as the Kemik Sandstone, pebble shale unit, and lowermost part of the Hue Shale (fig. 5). This included 10 samples through 37 ft (11.3 m) of the underlying Kemik Sandstone (Keller and Macquaker, 2001; Macquaker and Keller, 2005). In the Orion 1 well, Keller collected 86 samples from 83 ft (25.3 m) of the pebble shale unit and lower part of the Hue Shale (fig. 5). Core depths for all samples are reported in feet to minimize confusion when cross-referencing with the original core and related wireline log data (1 ft = 0.3048 m).

In the complete cored sections of the 2 studied wells, we picked the top of the pebble shale unit/base of Hue Shale based on the change in lithofacies described by Molenaar and others (1987) and Bird and Molenaar (1987, p. 51) as follows: "In outcrops, the upper contact is placed at the change from the generally nonbentonitic shale below to the interbedded shale and bentonite above." It is important to note that this contact based on lithofacies occurs above where it is placed based on the increase in gamma-ray log response in these wells (fig. 5) (Nelson and others, 1999, on Mikkelsen 1 well; Mickey and others, 2006, on Orion 1 well). The thickness of the lower part of the Hue Shale known as the GRZ is approximately 95 ft of a total Hue Shale thickness of 735 ft in the Canning River section (see figure SS2 in Macquaker and others, 1999). In the Mikkelsen 1 well, the GRZ is 172 ft of the 544 ft total thickness for the Hue Shale (Nelson and others, 1999). In the Orion 1 well, the GRZ is 74 ft of the 222 ft total for the Hue Shale (Kenneth J. Bird, USGS, oral commun., 2007).

We subsampled all hand specimens to make thin (20 µm), doubly polished thin sections for petrography and examination by SEM. These thin sections were investigated using combined optical and electron optical (backscattered electron imagery) techniques to determine the lamina and bedding geometries, minerals present, and the paragenetic relationships between cements (see Keller and Macquaker, 2001; Keller and others, 2001; Macquaker and Keller, 2005; and Macquaker and others, 2010, for more details on these methods). Where variations in backscatter coefficient were insufficient to unequivocally distinguish between minerals, we used energy dispersive spectrometry (EDS) to confirm mineral identifications, especially for carbonate cement. Additionally in the Mikkelsen 1 well, organic geochemical analyses were done, including Rock-Eval pyrolysis and carbon (C) isotopes for all samples (Keller and others, 2001; Macquaker and Keller, 2005) and a complete suite of biomarker analyses for six samples each from the pebble shale unit and Hue Shale (Paul G. Lillis, USGS, written commun., 2008; see also Keller and others, 2009).

Age control for the two wells is from biostratigraphic analysis by Michael B. Mickey and Hideyo Haga, Micropaleo Consultants, Inc.. Data and interpretations for the Mikkelsen Bay State 1 well are from Michael B. Mickey (written commun., 2000; see results in Keller and Macquaker, 2001) and for the Orion 1 well from Mickey and others (2006). For the Canning River section, age data is primarily from biostratigraphy supplemented by several 40Ar/39Ar ages on volcanic ash units within the Hue Shale from Steve Bergman (written commun., 1998; see also Macquaker and others, 1999).

The terminology used to describe mudstone lithofacies is from Macquaker and Adams (2003). In this system, which relies on the relative importance of the grain size of the main constituents, the mineralogy, and the presence of any diagnostic fabrics, "some" is used for constituents less than 10 percent, "bearing" is used for constituents greater than 10 percent but less than 50 percent, "rich" is used for constituents greater than 50 percent but less than 90 percent, and "dominated" is used for constituents greater than 90 percent. We made estimates of percent constituents using standard diagrams (for example, Harwood, 1988, p. 117) applied primarily to thin sections after first identifying finer grained components with SEM and by using EDS with SEM. Diagnostic fabrics such as "laminated" or "bioturbated" are mentioned first followed by significant mineralogy and grain size. For example, in this system a burrow-mottled mudstone composed of 5 percent pyrite plus 35 percent clay and 60 percent silt-size particles that are predominantly quartz and clay minerals (that is, what many geologists might refer to as a siltstone) would be described as a "bioturbated clay-bearing, silt-rich mudstone with some pyrite." To aid facies descriptions the silt- and sand-sized components likely present in the sediment before burial are described as being "framework" components, in contrast to the matrix component which is the less than 4 µm clay-sized material. In addition, we distinguished whether sediment constituents were likely derived from clastic inputs of sand, silt, and clay to the basin or from processes of either primary biological productivity (for example, radiolaria, foraminifera, calcispheres) or diagenesis (primarily pyrite and carbonate cement precipitated in the sediment after deposition; for example, Raiswell, 1988). The texture, constituent components, mineralogy, and grain size of mudstone samples are mainly evident from thin-section scans and optical petrography combined with SEM. Therefore, in the intervals between samples the lithofacies have been determined from core study and photographs in combination with extrapolation from adjacent samples.

Lithofacies and Textures

Lithofacies and lithofacies relations for the three studied sections are described below and shown schematically in figure 5. Sedimentary fabrics, structural and textural characteristics, and observed biogenic and diagenetic constituents are also described. In addition, figure 5 provides a gamma ray log for the two wells studied. Other log data for the Mikkelsen 1 well is provided in Keller and others (2001). For the Emerald Island section of the Canning River, the complete stratigraphic log plus gamma ray log are given in Macquaker and others (1999).

Muddy Sandstones and Sand- and Silt-Bearing Clay-Rich Mudstones

Examples of muddy sandstones, and sand- and silt-bearing clay-rich mudstones are shown in figure 6. These facies are most common in the top part of the Kemik Sandstone and basal part of the pebble shale unit of the Mikkelsen Bay State 1 well and Canning River section, and in the basal part of the pebble shale unit of the Orion 1 well (fig. 5). These relatively coarse grained lithofacies contain significant quantities of sand and silt in addition to clay. Texturally these units are thin bedded, normally graded, and form couplets as much as 10 millimeters (mm) thick. Individual beds are either laminated or bioturbated (for example, *Chondrites* isp. and *Phycosiphon* isp.). Bioturbation is either restricted to laminae within individual beds or pervasive.

In the Kemik Sandstone of the Mikkelsen well, basal laminae of individual beds are composed of medium-grained muddy sandstones in contrast to the topmost laminae that comprise fine-grained muddy sandstones and sand- and silt-bearing clay-rich mudstones. The sand and silt in these units are predominantly composed of quartz, with some feldspar, glauconite (particularly at the contact between the Kemik Sandstone and pebble shale unit, fig. 6*B*) and rock fragments. The matrix consists of illitic clay, muscovite, some euhedral pyrite, and amorphous organic matter. Kaolinite infills grain dissolution porosity. Scattered throughout these units are rare, outsized (larger than both matrix and framework grains), coarse sand- to granule-sized grains (mainly of quartz with some rock fragments, fig. 6*A*–*C*) and rare agglutinated and calcareous foraminifers (fig. 6*A*). The basal part of the pebble shale unit typically includes mud-supported clasts of lithologies similar to the rock formations below. In the Orion 1 well, for example, sand- to pebble-sized clasts of argillite are present in the basal sandy mudstone, as well as in the interval overlying it.

Mudstones with Some Mud-Supported Clasts

Scattered throughout strata of the pebble shale unit and to a lesser extent in the Hue Shale are mudstones with some mud-supported (floating), fine sand- to pebble-sized clasts composed mainly of quartz with some rock fragments (fig. 7). These clasts may be clustered together in poorly sorted fabrics of sand and silt-bearing mudstones (fig. 6*A*, C; fig. 7*F*) or occur in crude basal sandy and silty laminae of fining upward couplets (fig. 7*B*). Typically these clasts are rare, prominent (because they are outsized), and scattered or isolated throughout most of the succession (fig. 7*A*, *C*, *D*, *E*). However, their presence is common enough that their absence is very distinctive in certain units, particularly in the clay dominated mudstones interbedded with thin ash-fall tuffs in the pebble shale unit of the Mikkelsen 1 and Orion 1 wells and more generally in our thin sections from the Canning River section. Although these clasts were observed in hand samples and on the outcrop at Emerald Island, they do not seem to have been representatively captured in our thin sections (which are

Figure 5. Diagram showing lithofacies and lithostratigraphy of Lower Cretaceous sections, Arctic Alaska. Depth scale in feet (ft). Lithofacies thicknesses are schematic, not to scale. Blue dots are sample locations. "W" indicates core that weathered significantly during storage. Note that the gamma-ray log response for both wells is shown along with our interpretation of the base gamma-ray zone (GRZ) based on the abundance of tuff/bentonite as defined by Molenaar and others (1987); see text for discussion. For the Emerald Island section where the GRZ occurs above our measured section, see Macquaker and others (1999) for the complete section. The Lower Cretaceous unconformity (LCU) occurs in the Orion 1 well as shown at the base of the pebble shale unit, and in the Mikkelsen Bay State 1 well at the base of the Kemik Sandstone (not shown). This unconformity is not present in the Emerald Island section. API, American Petroleum Institute. m, meters.

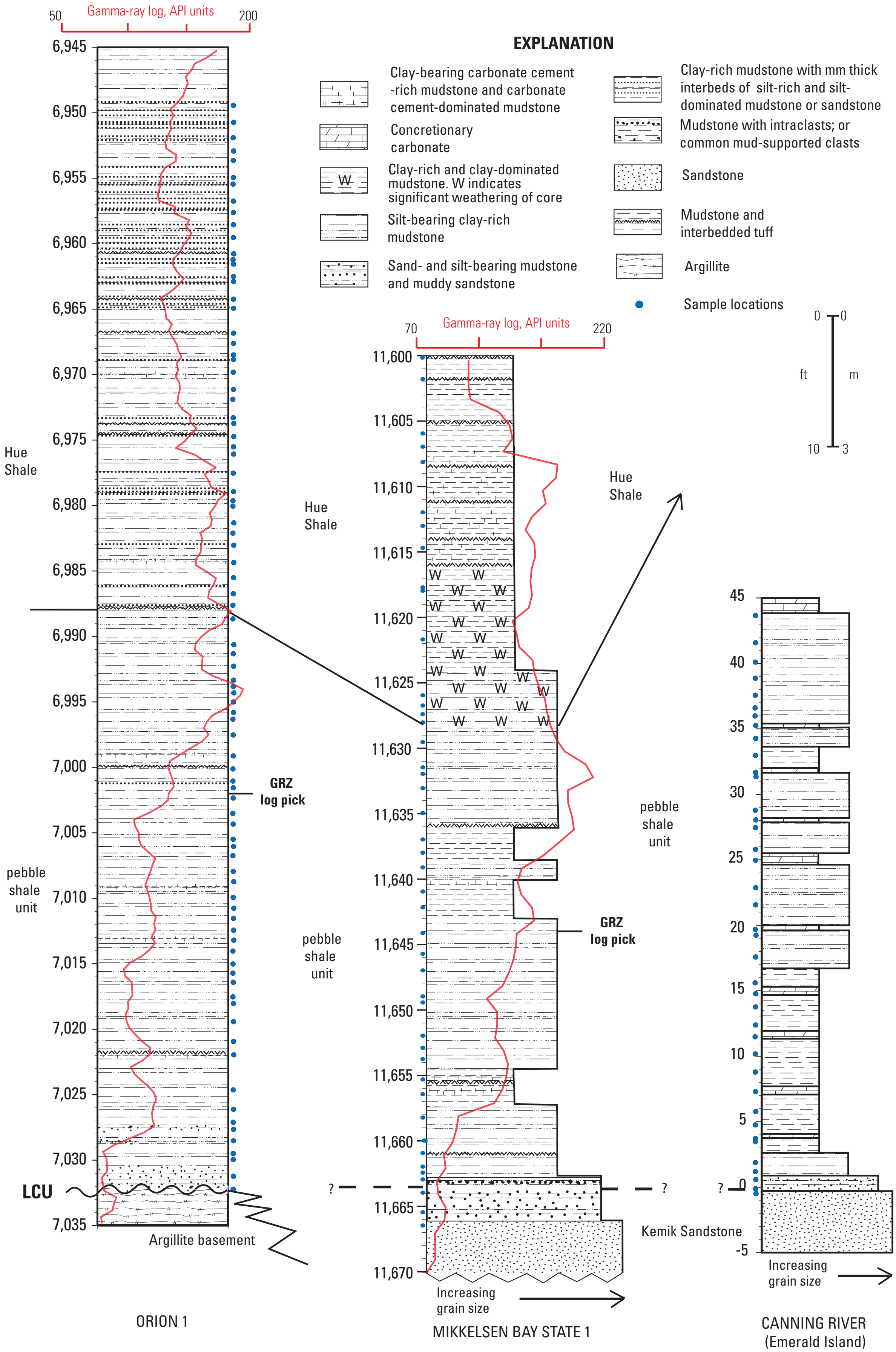

Gamma-ray log, API units
50
200
EXPLANATION
Clay-bearing carbonate cement -rich mudstone and carbonate cement-dominated mudstone
Concretionary carbonate
Clay-rich and clay-dominated mudstone. W indicates significant weathering of core
Silt-bearing clay-rich mudstone
Sand- and silt-bearing mudstone and muddy sandstone
Clay-rich mudstone with mm thick interbeds of silt-rich and silt-dominated mudstone or sandstone
Mudstone with intraclasts; or common mud-supported clasts
Sandstone
Mudstone and interbedded tuff
Argillite
Sample locations
Hue Shale
pebble shale unit
GRZ log pick
LCU
Argillite basement
ORION 1
70
220
Increasing grain size
Kemik Sandstone
MIKKELSEN BAY STATE 1
ft
m
CANNING RIVER (Emerald Island)

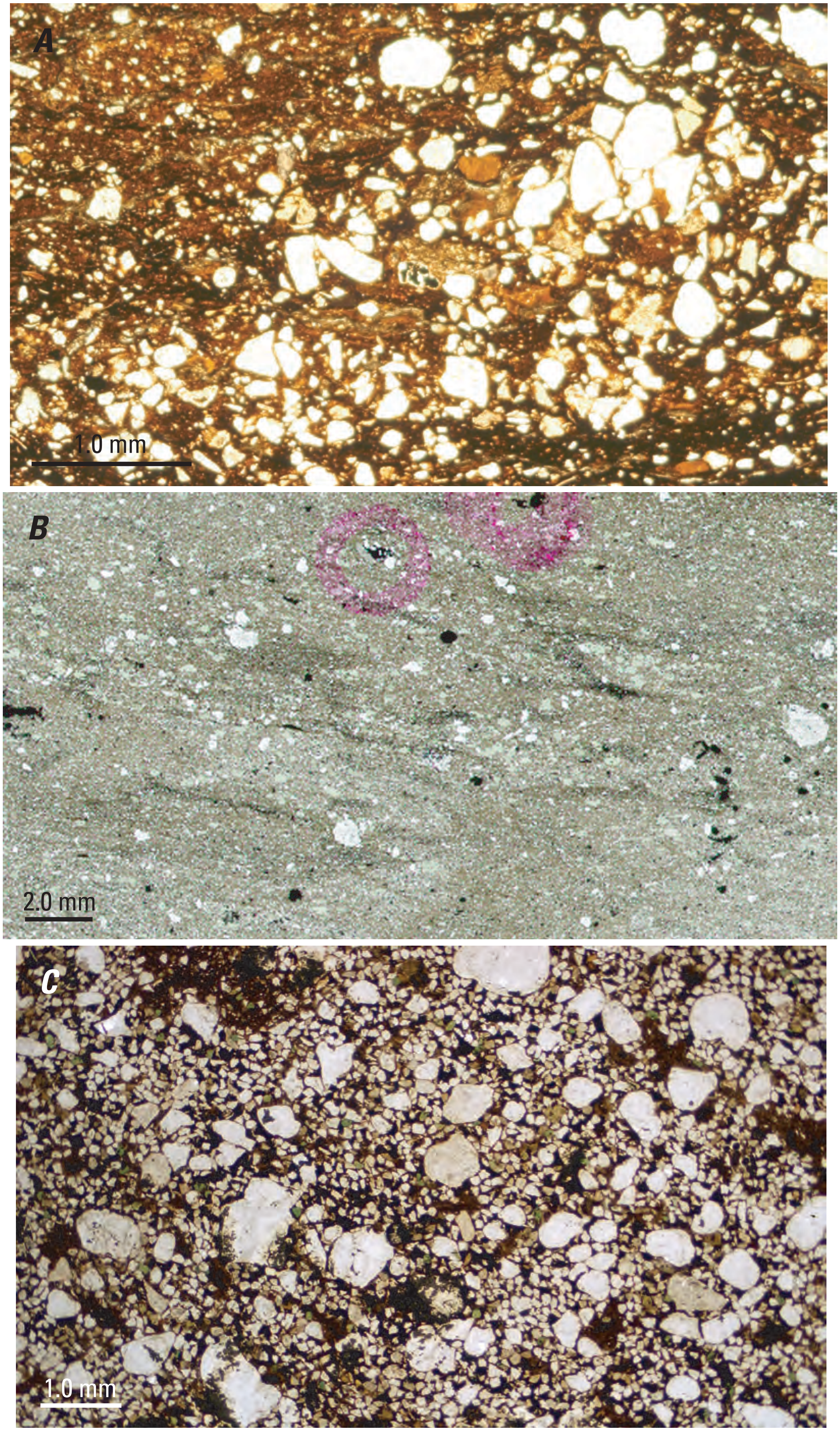

Figure 6. Photographs of sand- and silt-bearing clay-rich mudstones (*A*, *B*) and muddy sandstone (*C*) from Arctic Alaska showing variable bioturbation and other features in thin section scan (*B*) and photomicrographs (*A*, *C*) in plane-polarized light. *A*, Sample from the lower part of the pebble shale unit in the Orion 1 well at core depth 7,031.2 feet (ft) with pyrite infilled foraminifer in the center of image and poorly sorted cluster of fine to medium sand grains composed mainly of quartz with some rock fragments. *B*, Sample from the upper part of the Kemik Sandstone in the Mikkelsen Bay State 1 well at core depth 11,664 ft showing pervasive bioturbation attributed to *Phycosiphon* isp.; quartz and glauconite composition of the sand; and rare isolated, medium to coarse grained, mud-supported sand grains. Note that pink circles are indelible marks made on the thin section surface for the purpose of locating features with a scanning electron microscope. *C*, Sample from the lower part of the pebble shale unit at Emerald Island with bimodal sand grains that are medium to coarse, scattered rounded quartz grains and rock fragments in a matrix of mud and fine sand composed of quartz, glauconite, and rock fragments. mm, millimeters. (U.S. Geological Survey photographs by Joe H.S. Macquaker and Margaret A. Keller.)

composites from permafrost fractured outcrop). Also present are rare, mud-supported, rounded and pitted, fine-sand to silt-sized quartz grains (fig. 7*E*) (see Keller and Macquaker, 2001). In places, the streamlined tip of cone-shaped, mud-supported clasts appears to pierce and compress underlying laminae (fig. 7*D*), with overlying laminae draping the clast.

Silt-Bearing Clay-Rich Mudstones

Silt-bearing clay-rich mudstones, some with significant pyrite content (fig. 8), are commonly present throughout the Orion 1 well section and in the upper part of the pebble shale unit of the Canning River section sampled for this study. In the Mikkelsen 1 well they are the most abundant lithofacies of the pebble shale unit, common in the middle and top parts of the unit and also at the base of the overlying Hue Shale (see fig. 5). They are commonly associated with pyrite-bearing, clay-rich mudstones. Texturally, where not pervasively bioturbated, these silt-bearing clay-rich mudstones have very thin (0.5 to 5 mm) relict beds (fig. 8*A*–*E*). Within each bed, the constituent laminae consist of pellets or silt-enriched (in comparison with the pelleted laminae), partially flattened diminutive burrows (fig. 8 *A*–*E*). In some units significant quantities of framboidal pyrite (as much as 10 percent), with framboid sizes ranging from less than 5 µm to 30 µm, are present. Framboidal pyrite commonly defines relict-bedding planes (fig. 8*E*) and is abundant in the walls of some pellets (fig. 8*B*, *E*) (see also Macquaker and Keller, 2005). Within some silt-bearing, clay-rich mudstones in both the pebble shale unit and Hue Shale, silt-rich laminae with non-erosive bases form the base of upward-fining beds (fig. 8*A*, *C*, *E*). The silt in these laminae is commonly quartz and lithic grains. These silt-bearing clay-rich mudstones typically contain rare, scattered, mud-supported medium to coarse sand-sized grains (mainly composed of quartz), with very rare scattered agglutinated foraminifers and calcispheres (see Keller and Macquaker, 2001, and Macquaker and Keller, 2005).

Clay-Dominated and Clay-Rich Mudstones

Clay-dominated and clay-rich mudstones (fig. 9) occur predominantly in the Hue Shale although some intervals are present in the pebble shale unit, particularly associated with tuffs in the Mikkelsen 1 (fig. 9*D*) and Orion 1 wells, and in the lower part of the pebble shale unit of the Canning River section (fig. 5). These mudstones tend to have thin (5 to 10 mm), relict beds and contain laminae composed of pelleted and nonpelleted detritus. In some units, pelleted fabrics have been partially (fig. 9*C*, *E*) or completely (fig. 9*F*) destroyed by macrobioturbation (attributed to *Chondrites* isp.). These mudstones commonly contain small quantities (less than10 percent) of quartz silt, typically concentrated either at the base of individual lamina or in compressed silt-filled burrows as much as 0.5 mm in diameter. Rare mud-supported, medium to coarse sand grains (mainly quartz with some lithic grains) (fig. 9*A*, *C*), agglutinated foraminifers (fig. 9*F*), and calcispheres (fig. 9*D*) are also present.

Carbonate-Cemented Mudstones

Concretionary carbonate (fig. 2) and carbonate-cemented intervals (fig. 10) typically have much of their original fabric obscured by pervasive bioturbation (fig. 10*D* upper part, and *E*, *F*), but some intervals exhibit relict lamination or pelleted fabrics (fig. 10*A*–*C*). One carbonate-cemented interval has a few discrete borings that were made after cement formation (fig. 10*C*). Bedding is defined by the presence of carbonate, clay, and some silt interspersed with pyrite-rich layers (fig. 10*B*, *C*, *D*, *F*), or remnant, pellet-rich lamination (fig. 10*A*). In outcrop we refer to carbonate-cemented intervals as concretionary carbonate due to their morphology (figs. 2, 5). The carbonate cements are composed of microcrystalline, zoned dolomite and calcite (fig. 10*E*). The grains within the microcrystalline carbonate cement are mainly illitic clay, framboidal pyrite (many less than 10.0 µm), and amorphous organic matter, with minor silt and rare, isolated, sand-sized clastic grains.

In the lower part of the pebble shale unit of the Canning River section, 10 carbonate-cemented intervals range from 0.04 to 1.5 m thick (fig. 5; Macquaker and others, 1999). Carbonate-cemented intervals here are more numerous and thicker than in the pebble shale unit of the wells. Overall, carbonate-cemented intervals are thinner in the Orion 1 and Mikkelsen 1 wells compared to the Canning River section, and they are thinner and less common in the pebble shale unit compared to the Hue Shale.

Tuffs

In the Mikkelsen 1 and Orion 1 wells, tuffs and altered tuffs are present in both the pebble shale unit and the Hue Shale (fig. 5). In the Canning River section, tuffs are plentiful in the Hue Shale (described by Bergman and others, 1995; Bergman, 2006); however, no pure tuffs occur within the pebble shale unit there (Steve Bergman, written commun., 2006). Examples of tuffs and relict, pyrite-replaced tuffs from the studied wells are shown in figure 11 (see also Macquaker and Keller, 2005, figs. 4 and 6). In the pebble shale unit, tuffs are rare and thin, usually less than 5.0 mm thick, and are typically not obvious in hand specimen; some tuffs were collected as unidentified units within mudstone intervals (for example, fig. 11*D*, layer at base of image). They are primarily recognized in thin section and SEM by their angular grains (fig. 11*E*), texture, and composition [including feldspar and rock fragments that fine upward to clay (Macquaker and Keller, 2005)]. In the Hue Shale, tuffs and altered tuffs, including bentonites, are more abundant and thicker. Some are recognized from distinctive mineralized coatings on the core, such as jarosite, in addition to expansion and cracking of the core that formed by weathering during core storage.

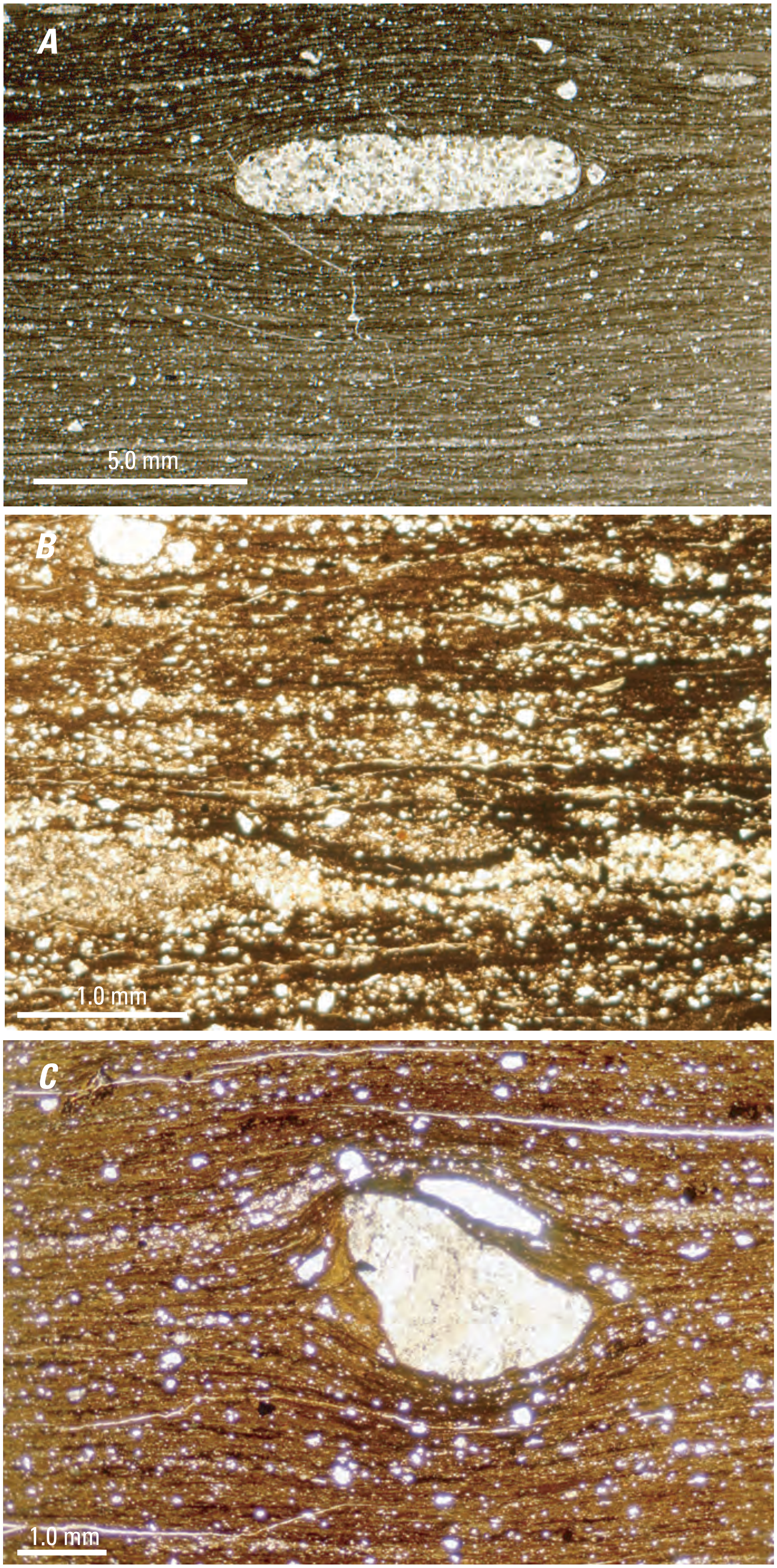

Figure 7. Photographs of rare, prominent, mud-supported, isolated, outsized (larger than framework and matrix grains), sand- to pebble-sized clasts representing "dropstones" (*A*, *C*–*E*), and more common, scattered large sand grains (*B*, *C*, *F*) in silt-bearing clay-rich mudstones from Arctic Alaska that have thin beds that commonly contain poorly sorted basal silt laminae (*B*, *C*). Also present are pelleted fabrics and rare to common, primarily bedding-parallel silt filled burrows—except in *F*, which is pervasively bioturbated. Photomicrographs *B*–*F* are in plane-polarized light; *A* is a thin section scan. *A*, Sample from the Hue Shale in the Orion 1 well at core depth 6,952.9 feet (ft) with well-rounded, elongate pebble, more common mud-supported sand grains and two larger silt filled, bedding parallel burrows (upper and lower right side of image) among many smaller burrows. *B*, Sample from the Hue Shale in the Orion 1 well at core depth 6,962.5 ft with scattered outsized, mud-supported sand grains and millimeter-scale genetic bedding that consists of basal silt-rich laminae that are crudely organized into thin bands, lenses, and pockets of silt with some sand that fine upward to clay-rich and clay-dominated, pelleted laminae. Some silt-rich laminae are disrupted by silt-filled burrows. *C*, Sample from the pebble shale unit in the Orion 1 well at core depth 7,020.9 ft showing scattered, more common mud-supported sand-sized grains and poorly sorted silt-rich laminae compressed at the base and draping over the top of "dropstone." *D*, Sample from the Hue Shale in the Mikkelsen 1 well at core depth 11,631.5 ft with a cone-shaped sand grain that has penetrated relict, clay-rich pelleted laminae bordered by pyrite. *E*, Sample from the pebble shale unit in the Mikkelsen 1 well at core depth 11,658.25 ft shows a prominent irregular, pitted quartz sand grain in lower right and abundant bedding parallel, silt filled microburrows as well as very long, apparently horizontal burrow in center of image. *F*, Sample is from 2.0 ft (0.61 meters) in the pebble shale unit at Emerald Island. Fine to coarse sand is composed mainly of quartz and some rock fragments. mm, millimeters. (U.S. Geological Survey photographs by Margaret A. Keller and Joe H.S. Macquaker.)

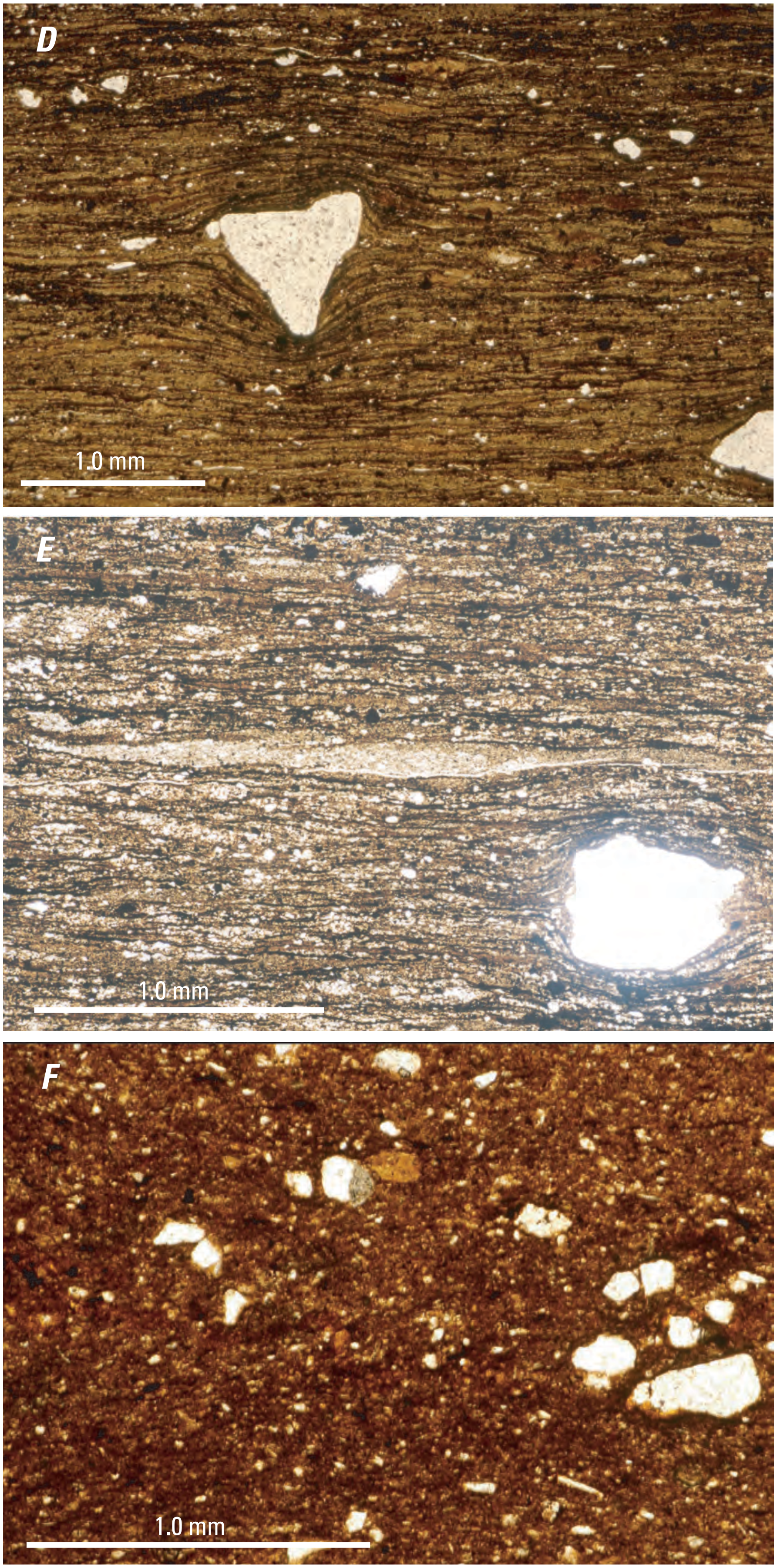

Figure 7.—Continued

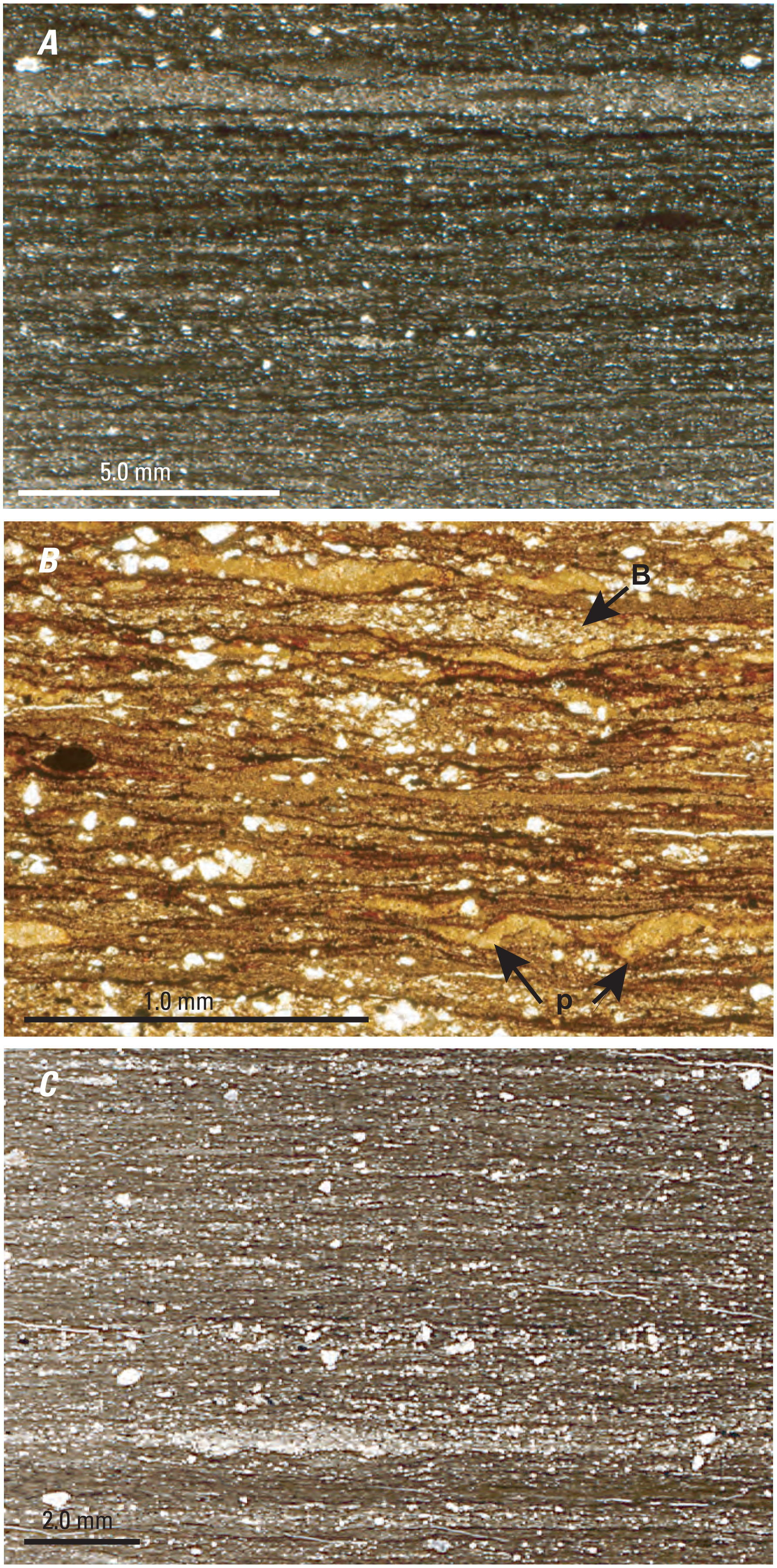

Figure 8. Photographs of silt bearing clay-rich mudstones from Arctic Alaska with partial bioturbation and thin relict bedding except for *F*, which is pervasively bioturbated. Photomicrographs *B*, *E*, and *F* are in plane-polarized light. *A*, *C*, and *D* are thin-section scans. *A*, Sample from the Hue Shale in the Orion 1 well at core depth 6,954.9 feet (ft) has millimeter-scale beds consisting of basal silt-rich laminae (modified by burrowing in places into wavy and crudely sorted lenses and thin layers) that fine upward to clay-rich and clay-dominated, pelleted laminae. Bedding parallel silt-rich and clay-rich burrows are common. *B*, Sample from the Hue Shale in the Orion 1 well at core depth 6,986.7 ft illustrates common clay-dominated fecal pellets (arrowed p) of different sizes and shapes, both clustered together and isolated, and also silt-rich lenses, burrows (arrowed B), and pellets (?). *C*, Sample from the pebble shale unit in the Orion 1 well at core depth 7,029.5 ft has bedding defined by subparallel thin, discontinuous clay-rich and silt-rich laminae, thicker and also burrow-modified laminae, rare continuous laminae, and particularly poorly sorted, coarser silt-rich lamina with sharp wavy basal contact and diffuse upper contact (3 millimeters, mm, from base of image). *D*, Sample from the Hue Shale in the Mikkelsen 1 well at core depth 11,629.6 ft shows common pyrite (arrowed Py) in thin subparallel black bands bordering thin clay-dominated and clay-rich laminae; rare thin discontinuous, disrupted, silt-rich laminae; and relatively larger bedding parallel oval burrows (arrowed B). *E*, Sample from the Hue Shale in the Mikkelsen Bay State 1 well at core depth 11,631.5 ft showing individual beds that have slightly wavy lower contacts (lower part of image) and silt-rich laminae (labeled S) at their bases that fine-upward (arrowed) into clay-rich pelleted laminae. The silt-rich laminae in the upper half of image are rarer, thinner, and discontinuous. *F*, Sample from 34.4 ft (10.49 meters) in the pebble shale unit at Emerald Island with pervasive bioturbation, some larger scattered mud-supported quartz sand and silt grains, and a foraminifer (lower left of center, arrowed F) that is probably agglutinated. (U.S. Geological Survey photographs by Margaret A. Keller and Joe H.S. Macquaker.)

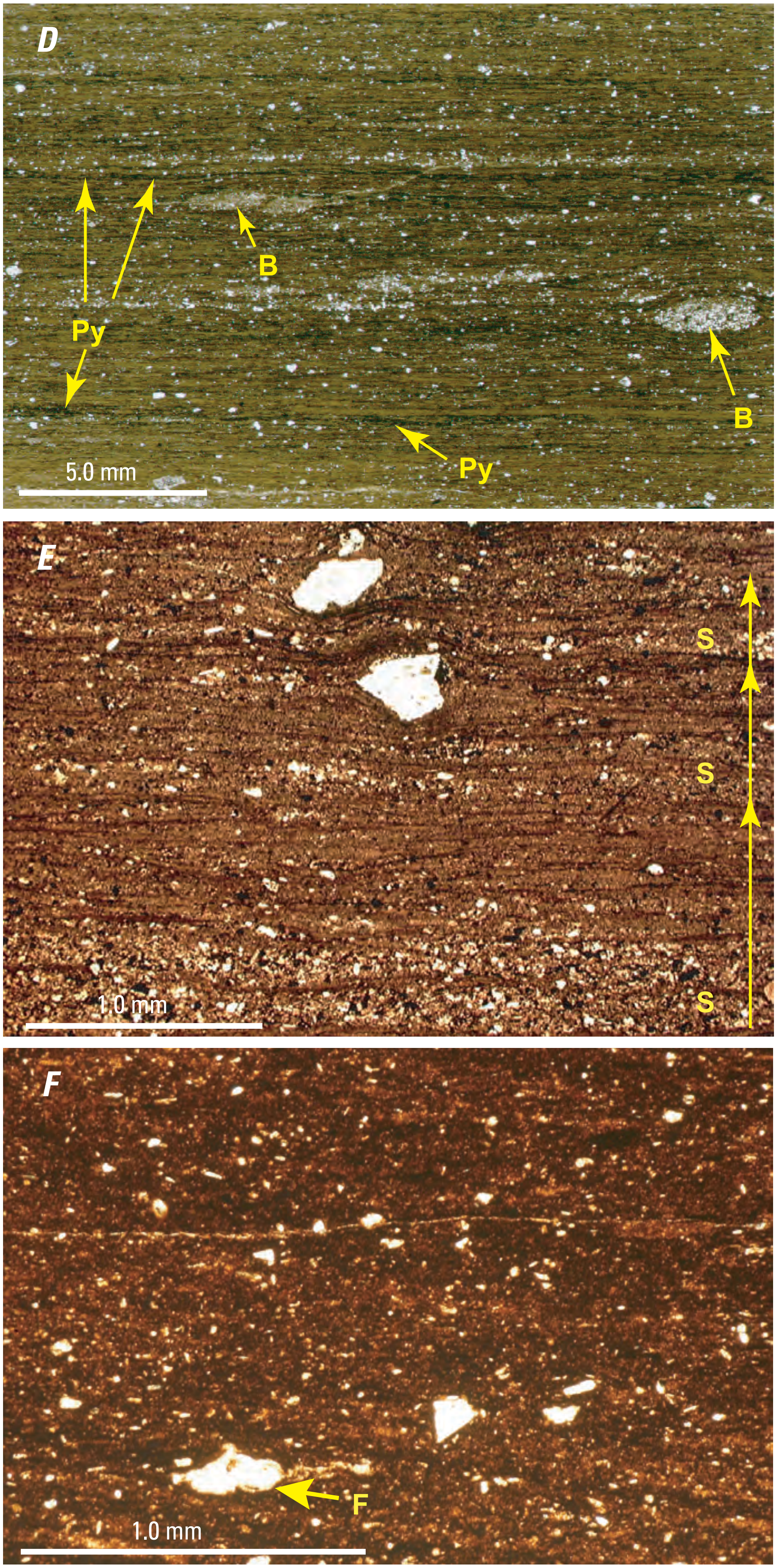

Figure 8.—Continued

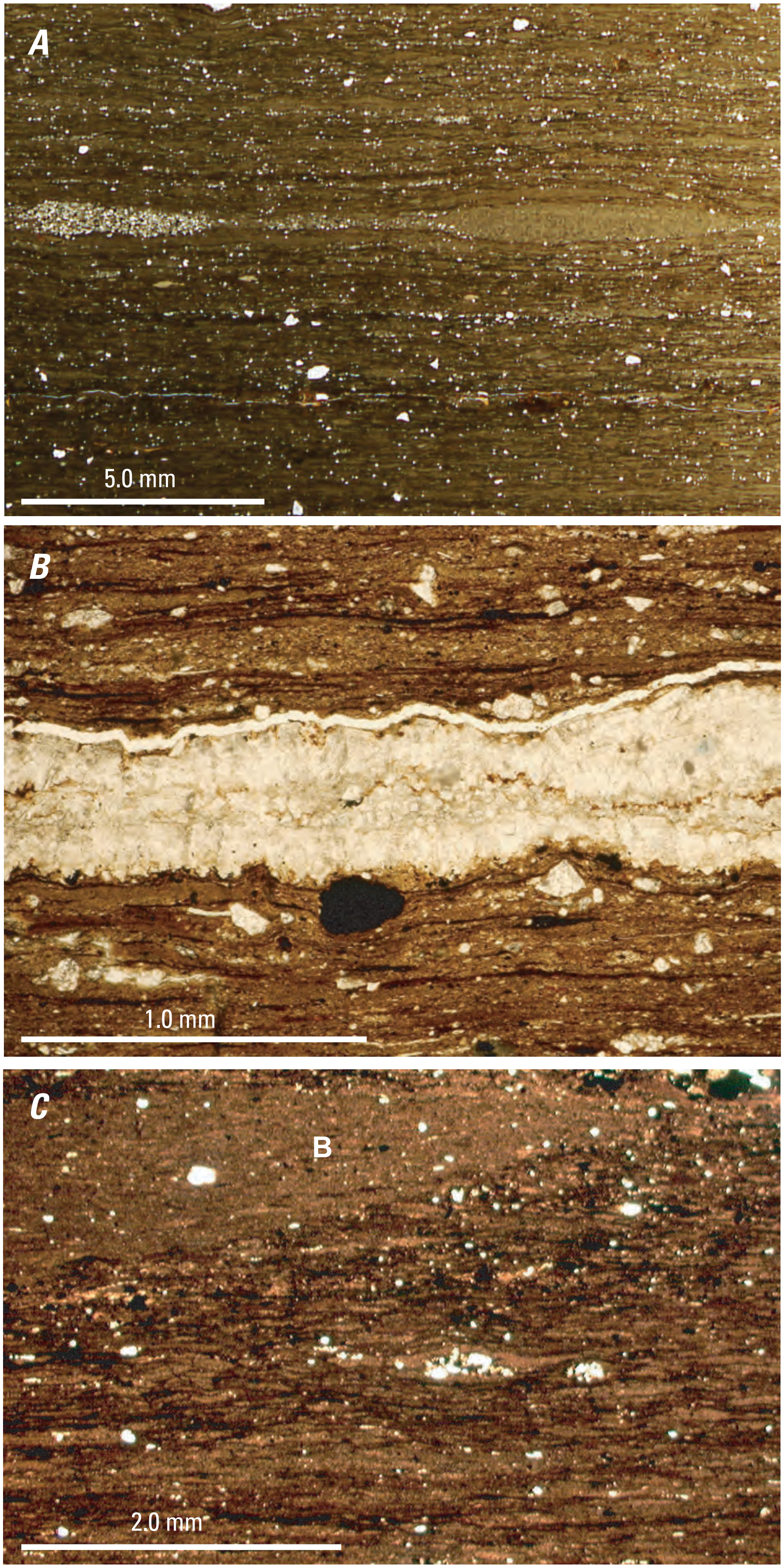

Figure 9. Photographs of clay-rich (*A*, *B*, *E*) and clay-dominated mudstones (*C*, *D*, *F*) from Arctic Alaska with horizontal burrows (*A*, *D*) and partial (*A*, *B*, *C*) to pervasive (*E*, *F*) bioturbation. *D–F* have relatively uniform-sized scattered silt and lack larger sand grains compared to *A–C*. Thin relict bedding and lamination are present in *A–D*, and pelleted fabrics are found in *A*, *C*, and *D*. Photomicrographs *B–F* are in plane-polarized light; *A* is a thin section scan. *A*, Sample from the Hue Shale in the Orion 1 well at core depth 6,984.3 feet (ft) with representative pelagic fabric comprised mainly of pellets between thin (one grain thick), discontinuous laminae of silt. Also present are rare scattered outsized grains of quartz sand and silt and large horizontal burrows filled with silt or clay-sized grains. *B*, Sample from the pebble shale unit in the Orion 1 well at core depth 7,007.9 ft with thin relict bedding; scattered, mud-supported quartz silt and sand grains and some pyrite (black) in thin, discontinuous, bedding-parallel bands and in a prominent well-rounded black grain; and very prominent bedding parallel band(s) of prismatic calcite from *Inoceramus* sp. *C*, Sample from the Hue Shale in the Mikkelsen Bay State 1 well at core depth 11,606 ft showing thin, relict-bedding, as well as cross-cutting lower boundary of a larger burrow (labeled B). Some pyrite and quartz sand and silt are present both in scattered and clustered grains. Pyrite is present in thin, bedding parallel laminae bordering some pellets. *D*, Sample from the pebble shale unit in the Mikkelsen Bay State 1 well at core depth 11,655.3 ft. Note distinctive pelleted fabric, some of which may be horizontal burrows (for example, Macquaker and others, 2010), with some scattered silt-sized quartz and pyrite. This sample contains 5.9-weight-percent total organic carbon (Keller and others, 2001). Very small spherical calcispheres (20–60 micrometers, µm, arrowed C) have a calcite rim and dark interior that is probably organic matter (Macquaker and Keller, 2005). *E*, Sample from 12.5 ft (3.81 meters, m) in the pebble shale unit at Emerald Island with prominent Y-shaped burrow (upper left and most of right side of image), as well as pyrite and scattered silt-sized quartz grains. *F*, Sample from 3.6 ft (1.10 m) in the pebble shale unit at Emerald Island with very rare, scattered silt-sized quartz grains, a possible agglutinated foraminifer (right of scale bar), and some pyrite. mm, millimeters. (U.S. Geological Survey photographs by Margaret A. Keller and Joe H.S. Macquaker.)

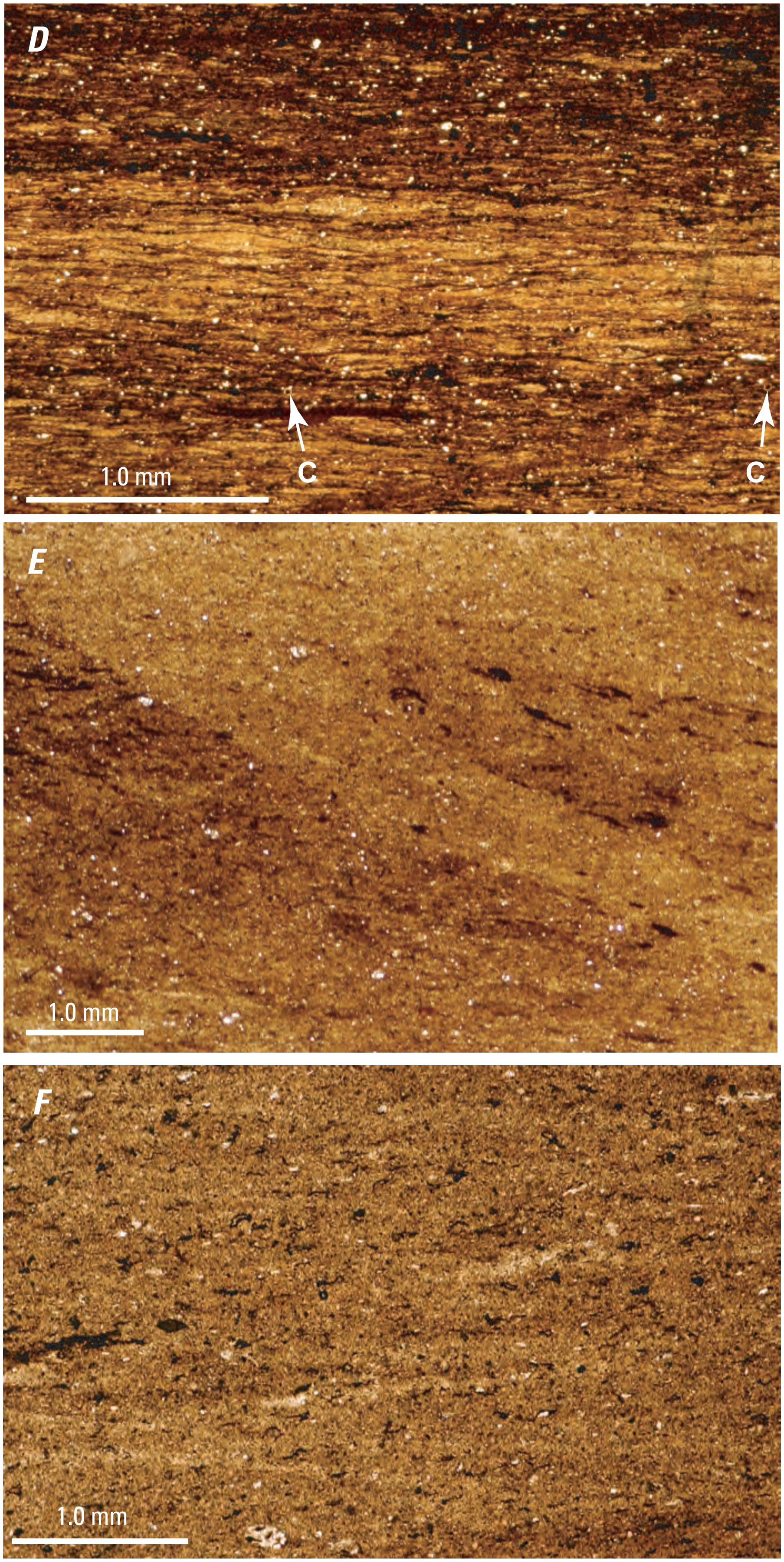

Figure 9.—Continued

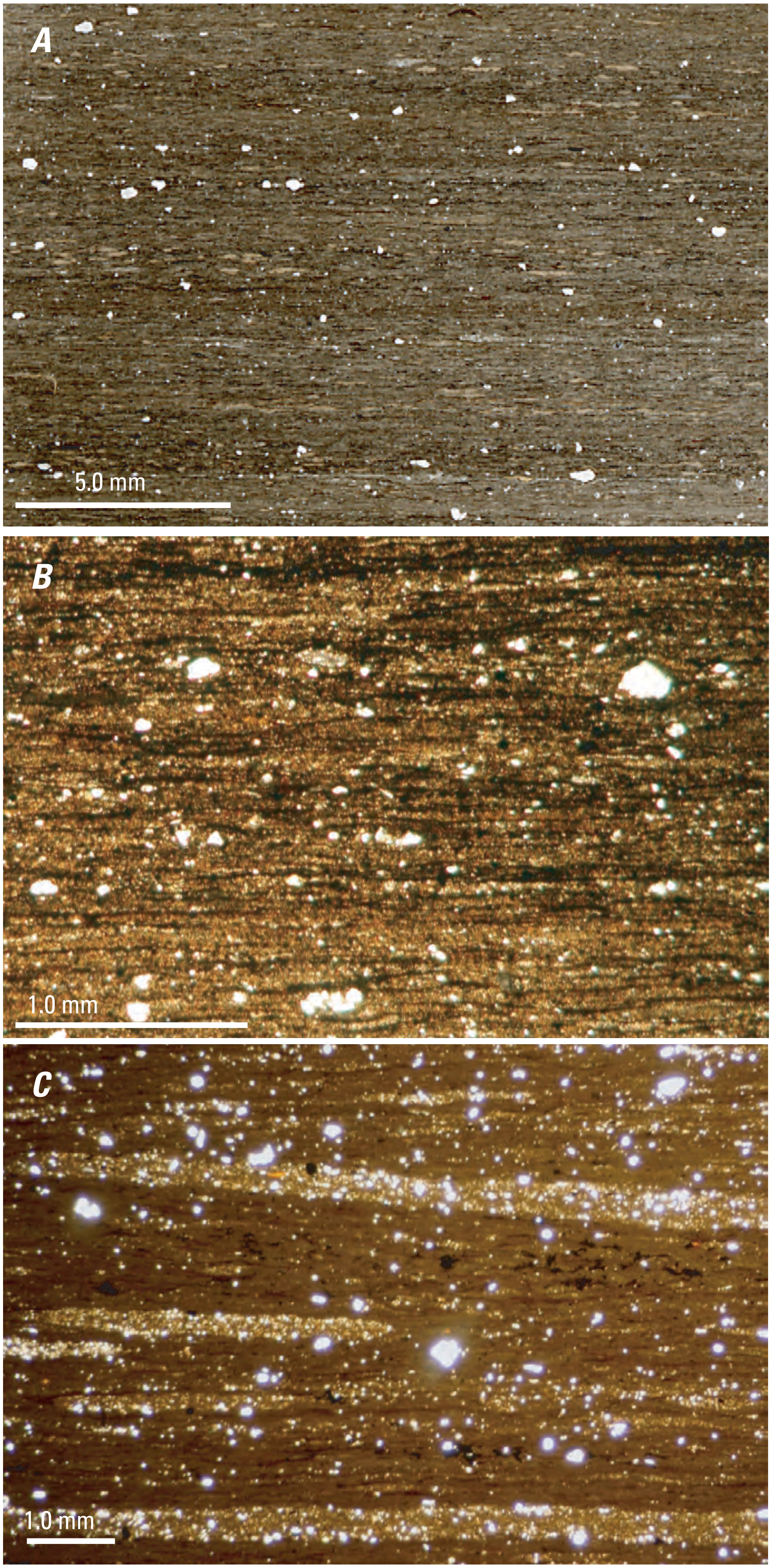

Figure 10. Photographs of clay-bearing carbonate-cement-rich mudstone (*A*, *B*, *E*, *F*) and carbonate-cement-dominated mudstone (*C*, *D* upper part) from Arctic Alaska showing relict lamination and pelleted fabrics (*A*–*D*) and variable but mainly limited bioturbation. Photomicrographs *B*, *C*, and *F* are in plane-polarized light; *A* and *D* are thin-section scans; and *E* is a backscattered electron image. *A*, Sample from the pebble shale unit in the Orion 1 well at core depth 6,999.06 feet (ft) with pelleted fabric that has thin relict lamination and some pyrite and scattered quartz silt and sand. *B*, Sample from the pebble shale unit in the Orion 1 well at core depth 7,013.7 ft showing thin relict lamination, some scattered mud-supported quartz sand and silt grains, and pyrite in thin bedding-parallel bands and silt-sized rounded grains. *C*, Sample from the pebble shale unit in the Orion 1 well at core depth 7,021.9 ft with horizontal to subhorizontal thinly laminated and bedded intervals at the top and base of the image and distinctive, bedding parallel borings that are siltier and lighter in color. Because these borings were made after carbonate cement formed, they have not been subsequently compacted. An interval in the middle of the image shows slightly crosscutting but similar lamination and prominent parallel borings. Original bedding—now diffuse and faintly visible due to carbonate cement formation—is mainly defined by very thin siltier laminae and pyrite. Also note scattered quartz silt and sand and some pyrite. *D*, Sample from the Hue Shale in the Mikkelsen Bay State 1 well at core depth 11,614.8 ft showing a lighter colored interval of bioturbated carbonate cement-dominated mudstone with some pyrite overlying a thinner interval of relict-bedded, pelleted and burrowed, pyrite-bearing clay-rich mudstone. Note that mud-supported, scattered quartz silt and sand grains are mainly present in zone where these 2 lithofacies meet and rare outside that zone. *E*, Sample from 11.6 ft (3.53 meters, m) in the pebble shale unit at Emerald Island with interlocking zoned calcite and dolomite rhombs in clay-bearing carbonate cement-rich mudstone. *F*, Sample from 7.4 ft (2.25 m) in the pebble shale unit at Emerald Island showing bioturbation; some pyrite in thin, probably bedding-parallel bands and irregular rounded grains; and quartz sand and silt grains. Rare isolated foraminifers (not shown) are present and also somewhat localized with pyrite between cemented intervals. mm, millimeters. µm, micrometers. (U.S. Geological Survey photographs by Margaret A. Keller and Joe H.S. Macquaker.)

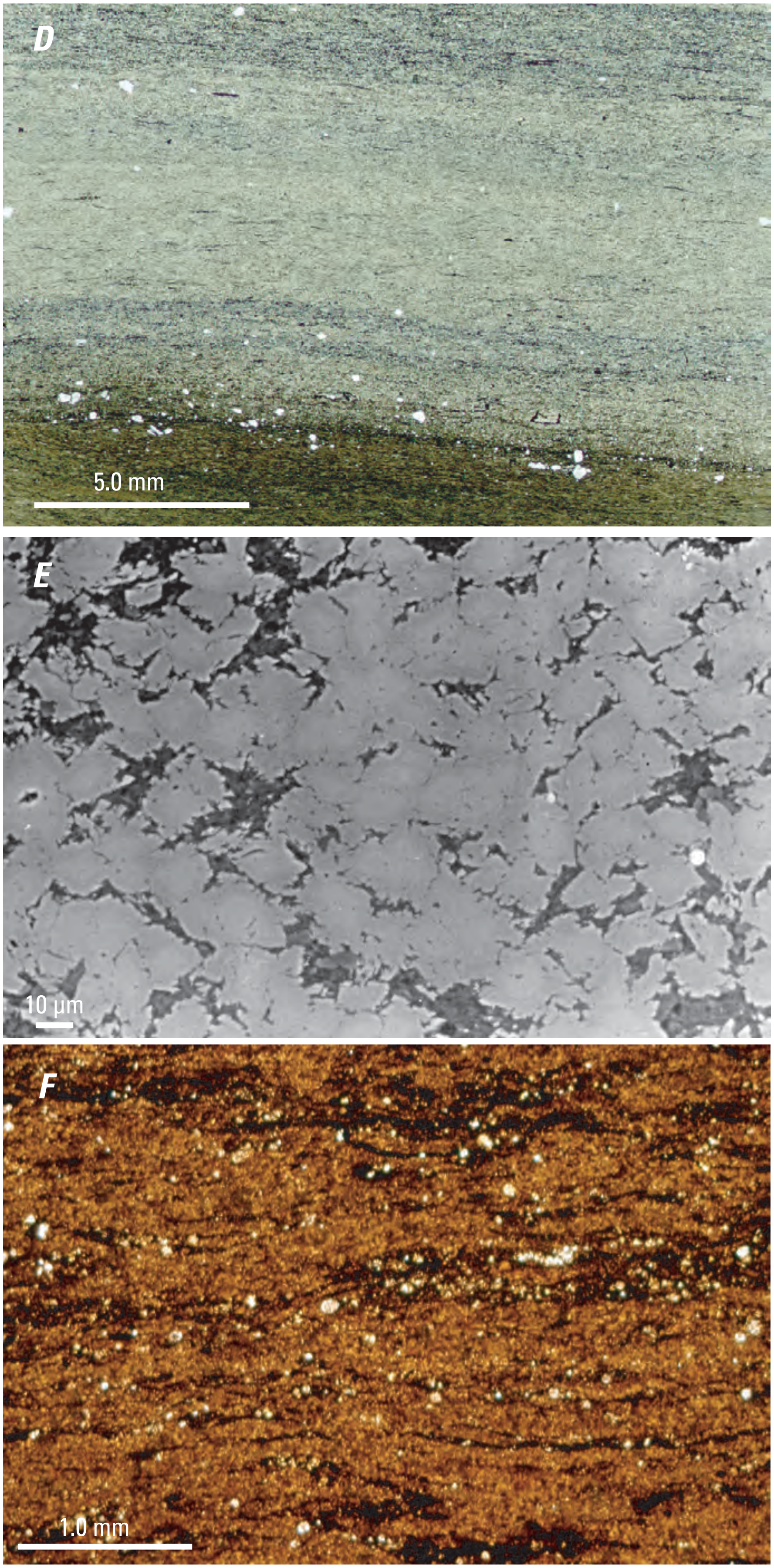

Figure 10.—Continued

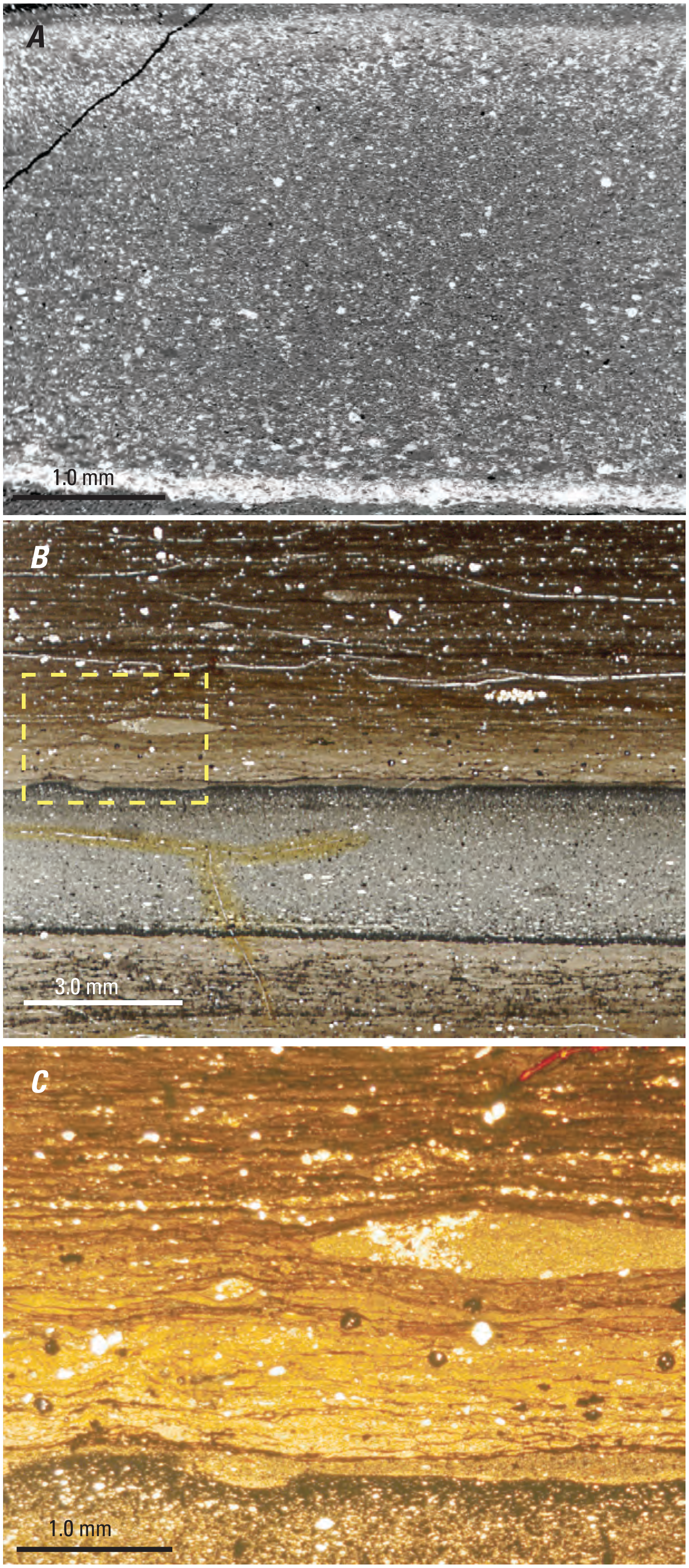

Figure 11. Photographs of graded tuffs (*A*, *B*, and *D*) and partially (*A*–*C*) to extensively pyrite-replaced, relict tuffs (*D* and *E*) interbedded with pelleted, clay-rich and clay-dominated mudstones from Arctic Alaska. *C* and *E* are photomicrographs in plane-polarized light. *B* and *D* are thin-section scans. *A* is a scanning electron microscope (SEM) backscattered electron image of the same tuff shown in *B*. *A*, Sample from the Hue Shale in the Orion 1 well at core depth 7,000.1 feet (ft). This backscattered electron image of a graded tuff highlights the occurrence of pyrite (in white, high h [density]) throughout the tuff, and shows a greater amount of pyrite mineralization/cementation in both the upper and lower parts of the tuff. *B*, Sample from the Hue Shale in the Orion 1 well at core depth 7,000.1 ft. The graded tuff (same as shown in *A*) in the lower half of this thin section scan is interbedded with pelleted, clay-rich and clay-dominated mudstones. In this image the pyrite is black. The yellow dashed rectangle shows the location of the enlarged image in *C* which highlights the pelleted and burrowed fabric overlying the tuff and bioturbation along the uppermost part of the tuff. *C*, Sample from the Hue Shale in the Orion 1 well at core depth 7000.1 ft showing a magnified view of the burrowed upper part of the graded tuff in "*B*", a larger burrow above the tuff, and the overlying pelleted, clay-dominated mudstone. *D*, Sample from the pebble shale unit in the Mikkelsen Bay State 1 well at core depth 11,655.3 ft showing a graded tuff (labeled "T") at the base of the interval shown. At least three relict and extensively pyrite-replaced, thinner tuff beds (black layers labeled "t") occur above the basal tuff interbedded with pelleted clay-dominated mudstone (see fig. 9*D* for enlarged photomicrograph from the middle of this image). Also, scattered quartz sand and silt grains occur in an interval above the basal tuff as well as localized in a lamina above the second tuff and otherwise are absent to extremely rare. *E*, Sample from the pebble shale unit in the Mikkelsen Bay State 1 well at core depth 11,661 ft showing prominent relict tuff unit, mostly replaced by pyrite (black) except for angular quartz and feldspar grains near base. Scattered quartz silt and pyrite in various forms are present in pelleted clay-rich mudstone above and below tuff. mm, millimeters. (U.S. Geological Survey photographs by Joe H.S. Macquaker and Margaret A. Keller.)

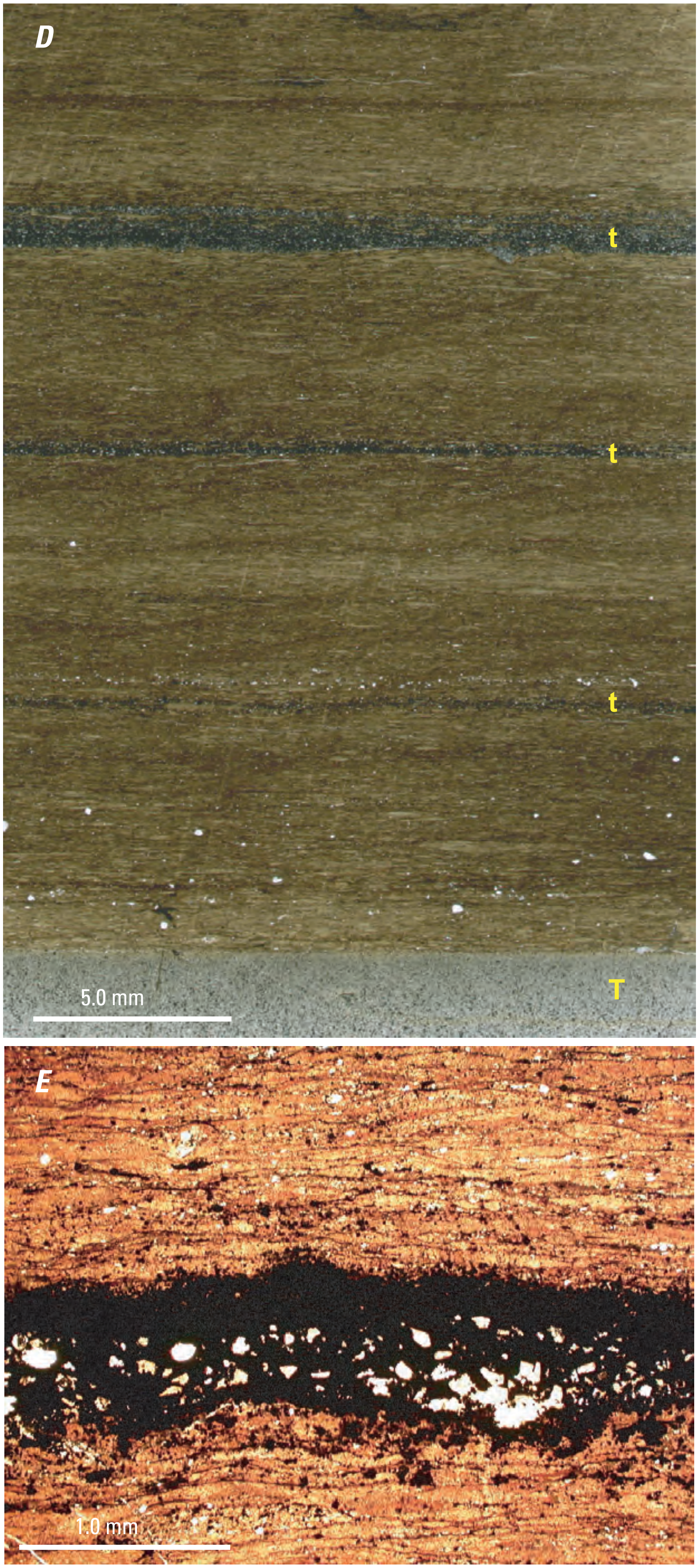

Figure 11.—Continued

In the Mikkelsen 1 well, the lowest volcanic ash is a relict tuff, almost completely replaced by pyrite, occurring at core depth 11,661.0 ft in the lower part of the pebble shale unit (figs. 5 and 11*E*). The next ash unit above this is a graded tuff with at least three very thin pyrite-replaced relict tuffs above it (fig. 11*D*). These thin pyritized tuffs define some of the original bedding. Similarly in the Orion 1 well, the lowest observed ash is a relict tuff in the lower part of the pebble shale unit at a core depth of 7,021.9 ft (fig. 5).

In the Mikkelsen 1 well, tuffs are particularly abundant above core depth 11,628 ft, where we placed the base of the Hue Shale. In this well, many intervals where tuffs are common have been extensively "weathered" during storage of the core (fig. 5, interval with "W"). Tuffs in the Hue Shale are commonly thicker (greater than 20 mm thick) than in the pebble shale unit and characteristically fine upward. Their bases comprise coarse sand-sized, angular feldspar and rock fragments that fine upward into clay. Although pyrite is commonly present throughout these tuffs (fig. 11*D* and *E*), either or both the top and base of tuff intervals are typically cemented more extensively by euhedral pyrite (see examples from Orion well, fig. 11*A* and *B*). Many of the larger grains at the base of individual tuffs have been replaced by authigenic kaolinite (Macquaker and Keller, 2005).

In the Orion 1 well, the base of the Hue Shale was placed at a core depth of approximately 6,988 ft (fig. 5), above which tuff and tuffaceous mudstones are more abundant and generally thicker. Commonly, pyrite either partially (see small black grains in groundmass of middle part of tuff shown in fig. 11*B* [white in backscattered electron image (BSE) of same tuff shown in 11*A*]) or extensively replaces these tuffs (see top and basal intervals of same tuff, fig. 11*A*–*C*). In some, the tops of individual units have also been somewhat disrupted by bioturbation (fig. 11*B* and *C*). In addition to agglutinated foraminifers and radiolaria (Mickey and Haga, written commun., 2000), calcispheres are particularly abundant in some units associated with the tuffs in the Mikkelsen 1 well (fig. 9*D*) (see Keller and Macquaker, 2001; Macquaker and Keller, 2005).

Sandstone and Silt-Rich and Silt-Dominated Mudstone in the Orion 1 Well

Thin millimeter- to centimeter-scale laminae of sandstone and sand-bearing silt-rich and silt-dominated mudstone are common in some intervals of the Hue Shale in the Orion 1 well but rare in the pebble shale unit (figs. 5, 12). These sediments form distinctive intervals of millimeter-scale beds/couplets (figs. 12*C*, *F*) consisting of basal laminae of fine to very fine sand-bearing silt-rich and silt-dominated mudstone that fine upward to clay-dominated laminae. Some of these laminae that are not well sorted may be slightly coarser grained equivalents of the silty-based, crudely sorted, fining upward beds/couplets present in the Hue Shale of the Mikkelsen 1 well (figs. 8*E*, *D*). In that well, this lithofacies is present, but rare in both the pebble shale unit and the Hue Shale, and the coarse, basal laminae are typically less than or equal to1 mm in thickness.

Two thicker intervals of sandstone are also present in the Hue Shale in the Orion well (fig. 12*A*, *B*, *D*, *E*). The older of these occurs at a core depth of 6,962.9 ft, is 1.5–2 cm thick, and consists primarily of graded, planar-laminated, thin sandstone, sand-bearing, silt-rich and silt-dominated mudstone, and thinner clay laminae (fig. 12*E*) deposited on a scoured angular contact with the mudstone below. The upper part of this mudstone has a unique fabric similar to that of the pebble shale unit with lenses and pockets of poorly sorted coarse sand in mudstone (fig. 12*B*). The younger sandstone interval is massive, fine-grained, 10 mm thick, and occurs at a core depth of 6,950.7 ft. It has a gradational/diffuse contact zone with the overlying, silt-bearing, clay-rich mudstone in which the basal part of the mudstone has incorporated (plucked up) grains of the sand (figs. 12*A*, *D*) during deposition of the flow that deposited the overlying mud.

Lithofacies, Sequence, and Other Characteristics

Petrographic and SEM results indicate that the Lower Cretaceous succession at each of the three studied sections consists primarily of clay-rich mudstones that are variously sand- or silt-bearing and clay-dominated mudstones with as much as about 10 percent silt and sand. What differs between the studied sections are the proportions of these mudstone lithofacies, the carbonate-cemented intervals, and the other lithofacies such as tuff or sandstone present at each location. A distinctive, much coarser unit of pebbly to sandy mudstone and muddy sandstone for which the pebble shale unit is named is commonly present at the base of these sections. Pebbles and coarser clasts are commonly more abundant in the lower part of the pebble shale unit, particularly in pebble lags at the base of the unit. Also distinctive and common throughout the pebble shale unit, but less so in the Hue Shale, is a lithofacies characterized by outsized, mud-supported sand-sized grains with rare granules and pebbles. These occur either as isolated clasts or in poorly sorted clusters throughout much of the studied succession, but are rarer in the Hue Shale.

Variable amounts of other lithofacies are present within the succession including, carbonate-cemented mudstone, tuff/bentonite and tuffaceous/bentonitic mudstone, sandstone, and pyrite-bearing mudstone. These lithofacies are present with different abundance and stacking patterns in all three sections with two exceptions. Thin tuff and probable tuff intervals are present in the pebble shale unit of both wells but were not observed in the pebble shale unit of the Canning River section. Secondly, discrete intervals in the Hue Shale of the Orion 1 well contain abundant, millimeter-thick beds with basal laminae of sand-bearing, silt-rich and silt-dominated mudstone and fine-sandstone that fine upward to clay-rich and clay-dominated laminae and in addition contain several thicker sandstone and silt-dominated mudstone intervals. These coarser grained and better sorted lithofacies were rarely observed in the pebble shale unit or in the other Hue Shale section we studied. Where they occur in the Orion 1 well, they are distinguishable within a dominantly mudstone succession that overall fines upward from the pebble shale unit into the Hue Shale. Individual genetic beds (from the same depositional event; 2–5 mm thick) in the pebble shale unit are commonly more crudely bedded and poorly sorted in contrast to thin, well-bedded and primarily well-sorted strata in the Hue Shale.

Some of the mud-supported, sand-sized component is notably rounded and pitted (Keller and Macquaker, 2001; Macquaker and Keller, 2005). The occurrence of clasts with these characteristics is quite variable and has been quantified for grains greater than 74 mm as the number of "rounded frosted quartz floaters" (RFQF) [for example, Mickey and others (2006) for the Orion and many other wells; see also Mike Mickey, written commun., (2000) in Keller and others (2001) for the Mikkelsen well].

Variable bioturbation is present throughout the succession, most commonly as bedding-parallel, diminutive or microbioturbation that appears to disrupt otherwise continuous laminae. Burrows (fig. 9*C*) and borings (fig. 10*C*) also crosscut multiple laminae in places. Pervasive bioturbation (figs. 9*E* and *F*) and macrobioturbation (figs. 9*C* and *E*) by *Chondrites* isp. and *Phycosiphon* isp. are rare. A distinctive pelleted fabric (for example, figs. 9*A* and *D*, 10*A* and *B*, and 11*C–E*) occurs in many of the clay-dominated intervals, particularly associated with ash-fall tuffs. In some thin sections where burrows do not cut through more than one layer, the distinction between burrows and pellets is equivocal. For example, it is evident in a sample from the Mikkelsen well that branching, horizontal burrow morphologies are present in a thin section cut parallel to bedding in which the bedding is defined by multiple "pellets" (Macquaker and others, 2010).

It is noteworthy that the tuffs in both formations in the wells are associated with fecal pellets of clay and organics in laminated intervals containing very little siliciclastic detritus. One of these pelleted samples in the Mikkelsen 1 well occurs within an interval that contains the greatest numbers of both radiolaria and agglutinated foraminifers (Mike Mickey, written commun., 2000) and also shows the highest petroleum source potential of the Lower Cretaceous succession in that well (Keller and Macquaker, 2001; Keller and others, 2001). Mickey and others (2006, and references therein) have also documented radiolaria (sometimes including abundant pyritized forms), palynomorphs, dinoflagellates, calcareous and agglutinated foraminifera, rare mollusks including *Inoceramus*, and various other fossils and minerals in these and many other exploratory wells and outcrop sections across the North Slope and in exploration wells on the Beaufort Sea shelf. We observed rare calcareous and agglutinated foraminifera, calcispheres, and the bivalve mollusk *Inoceramus* in some thin sections.

Discussion

The biofacies, lithofacies, and lithofacies stacking patterns observed in these sections are interpreted to result from deposition in a marine setting where sediment was supplied primarily by fluvial sources with minor input from volcanic ash falls and aeolian processes. However, a mudstone lithofacies is present with outsized, mud-supported clasts (from fine sand to pebble size) that have a dropstone texture that is not explained by these sources and processes. These clasts are very likely to occur in a cold, high-latitude, marine setting where sediment-laden sea ice could form (Lisitzin, 2002).

Early in our investigation of the Lower Cretaceous succession of the North Slope, only a few authors (Mull, 1987; Scotese and others, 2001; Spicer, 2002) had suggested that the sections we were studying had been deposited at high latitude, similar to their present positions at approximately 70° North. Additionally, the implications of this setting for sedimentary processes and resulting lithofacies and organic facies had not been evaluated. Therefore, we investigated modern climate and sedimentary processes occurring in the Arctic as possible analogs for understanding and interpreting the Lower Cretaceous lithofacies, organic facies, and sedimentary fabrics of these sections we studied. This is important because research in the past two decades on Cretaceous floras, faunas, and depositional environments indicates that the climate was highly variable, and sometimes cold, at high latitude in the Arctic during that time (Zakharov, 1994; Price and Mutterlose, 2004).

Early Cretaceous Arctic Climate

Several studies using multiple lines of evidence discuss Early Cretaceous climate at northern high latitudes and either indicate that it was at least seasonally cold during part of the Hauterivian Stage or are consistent with that interpretation. For instance, on the North Slope of Alaska, glendonite was reported in Lower Cretaceous sediments by Kemper (1987) and more recently by van der Kolk and others (2007) and van der Kolk (2010) who reported the discovery of glendonite in the pebble shale unit near the Canning River. Glendonite is a calcite pseudomorph of ikaite ($CaCO3·6H2O$), which only forms at near-freezing temperature in waters of high alkalinity (for example, Frakes and Francis, 1988). Furthermore, Mull (1987, p. 412) indicated that the Kemik megafauna (Hauterivian-Barremian Stages) of the North Slope—as interpreted by R.C. Allison—has characteristics of a "boreal paleogeographic setting" that "suggests marginal living conditions for part of the Kemik fauna, possibly including seasonal ice."

On the basis of isotopic data collected from latest Jurassic-Early Cretaceous boreal belemnites from the Yatria River in Siberia, which show a shift to lower temperatures (the lowest "encountered from the late Valanginian—early Hauterivian

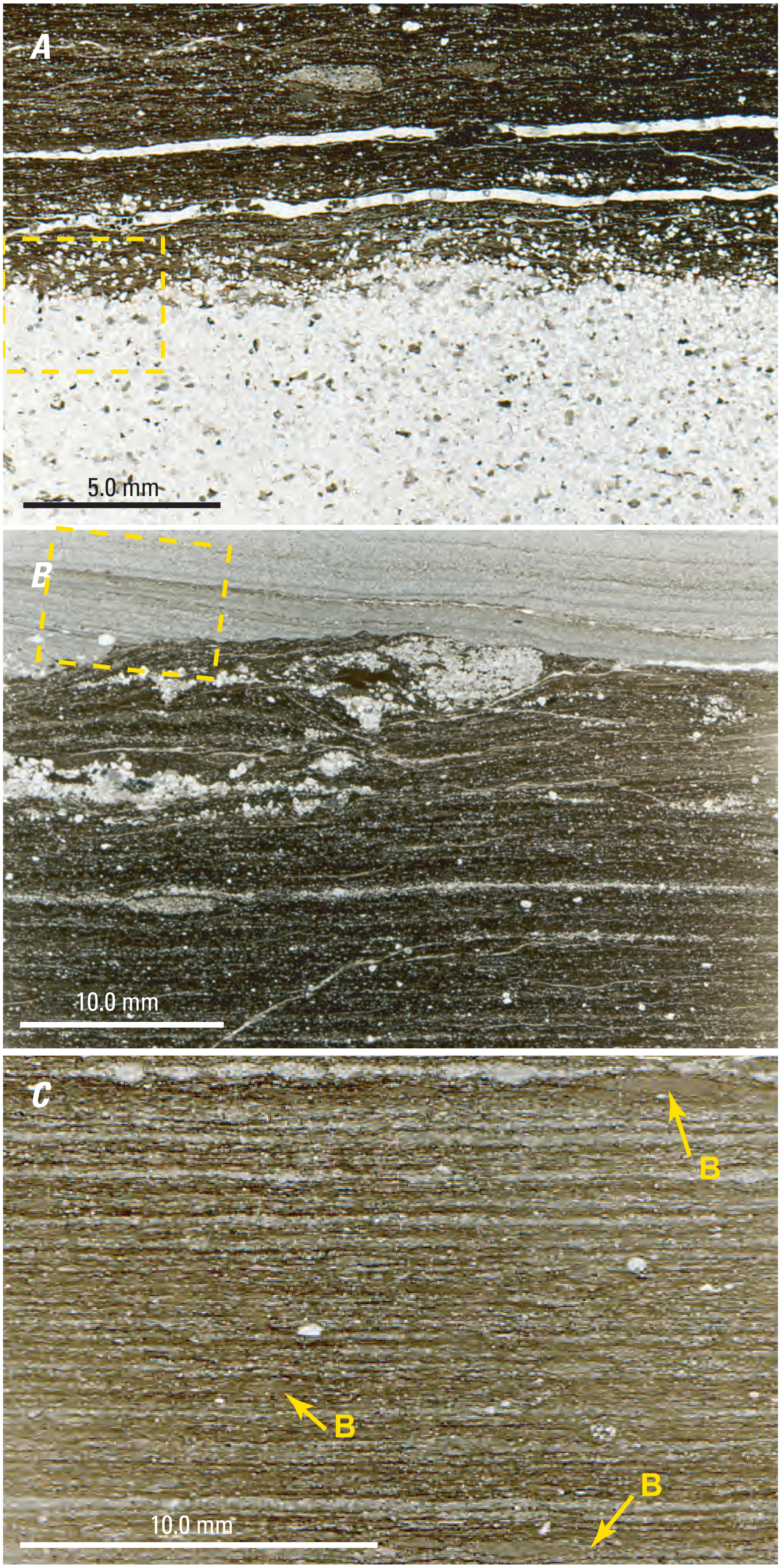

Figure 12. Photographs of sandstone and sand-bearing silt-rich mudstones in the Hue Shale of the Orion 1 well in Arctic Alaska. Paired thin-section scans (*A*–*C*) and photomicrographs (*D*–*F*) illustrate these coarser lithofacies. Yellow, dashed rectangles in *A* and *B* show location of photomicrographs in *D* and *E*. *A*, *D*, Massive, well-sorted, fine-grained sandstone 10 millimeters (mm) thick with primarily subrounded to angular grains of quartz, feldspar, and some mafic minerals and rock fragments. Upper contact of sandstone is very irregular and gradational as a result of sand grains in the upper part being incorporated into overlying silt-bearing clay-rich mudstone. Note zone of scattered, mud-supported sand grains in photomicrograph *D* taken with crossed polars. Sample from core depth 6,950.7 feet (ft). *B*, *E*, Thin, planar-laminated silt-rich and silt-dominated mudstones with minor, thin, sand-bearing silt-rich mudstone and clay-rich mudstone laminae overlying a scoured angular contact with predominantly silt bearing clay-rich mudstone below. Note lenses and pockets of poorly sorted coarse to fine sand in the upper part of this clay-rich mudstone unit as well as rare, isolated mud-supported sand sized quartz grains. Sample from core depth 6,962.9 ft. *C*, *F*, Partially bioturbated (elongate, bedding-parallel flattened burrows with tapering edges, arrowed "B"), thin-bedded, silt-bearing, clay-rich mudstone with silt-rich laminae forming the basal units of millimeter scale beds/couplets that fine upward to clay-dominated laminae. Many of the basal laminae are very thin (one or two grains thick) and many are not well sorted, containing some fine to very fine sand, as well as silt and very fine silt. Note wavy, irregular lower contact of upper, slightly coarser lamina/bed in *C*; numerous bedding-parallel burrows, and very rare scattered, outsized quartz sand grains and rock fragments; and silt-dominated lamina (labeled "S") below burrow (labeled "B") in *F*, which may have deformed/bent around this burrow during compaction to form wavy contact. Sample from core depth 6,977.5 ft. (U.S. Geological Survey photographs by Margaret A. Keller.)

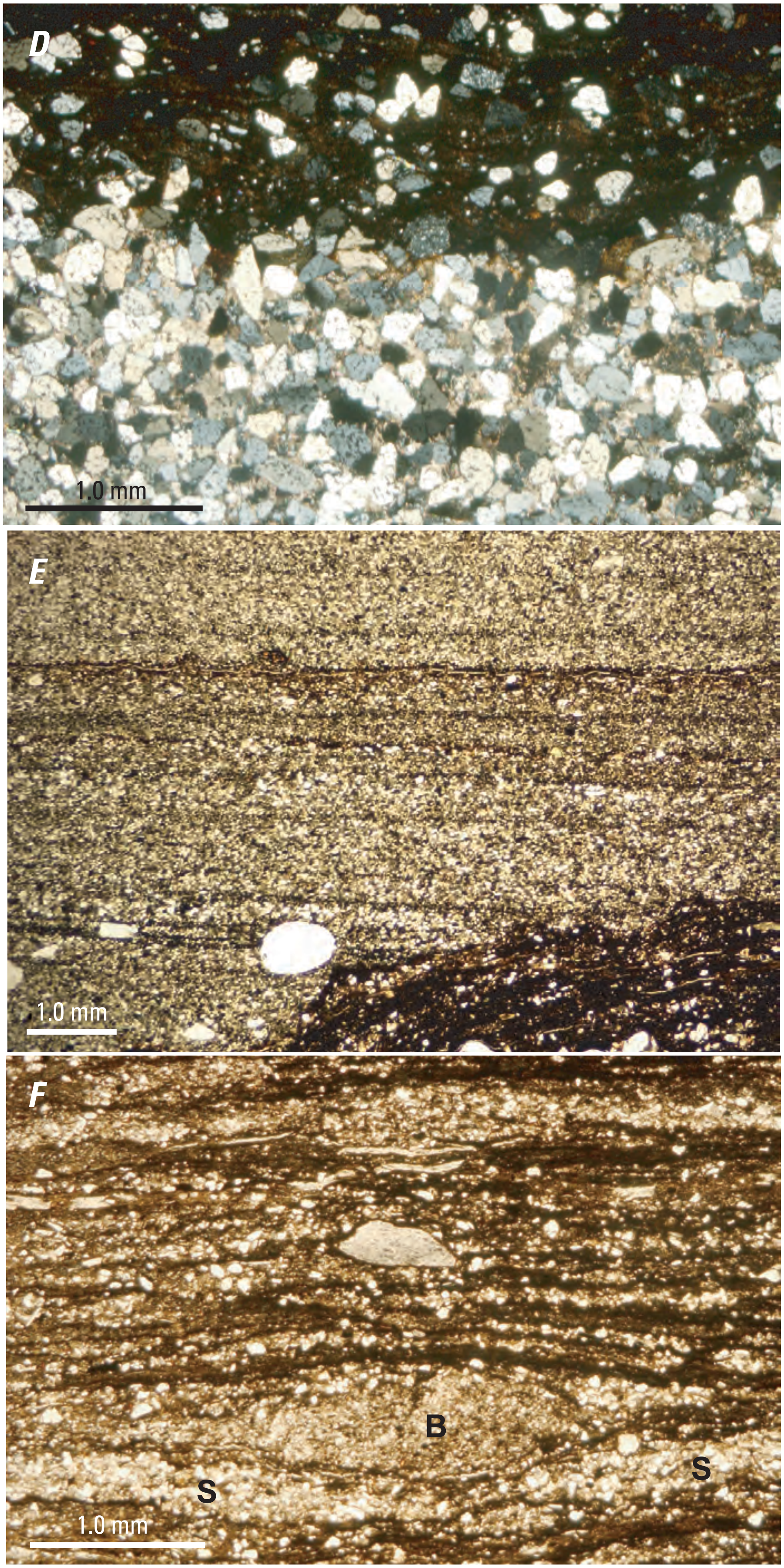

Figure 12.—Continued

Stages"), Price and Mutterlose (2004, p. 966) conclude "that low ocean temperatures are consistent with limited polar ice and suggest that the region was at times considerably colder than previously thought." In addition, Zakharov (1994, p. 25) describes the occurrence in a Lower Cretaceous succession in the Siberian Arctic of many glendonite concretions ("hedgehogs"); he also reports that his interpreted "climate curve falls rapidly in the Valanginian and reaches its lowest point for the whole Cretaceous in the early Hauterivian." These data are also consistent with overall fining and deepening upward of the succession in the Orion well (middle neritic through bathyal to distal depositional settings [Mickey and others, 2006]) in that—other things being equal—relative sea level would be expected to be lower when it is colder and more ice is present and then relatively higher as warming occurs and ice melts. Continued rifting in the Canada Basin would have also increasingly deepened the setting. Another line of evidence that is consistent with a relative rise in sea level/deepening is the extent of reworked Early Cretaceous palynomorph assemblages. Haga and Mickey (2002) indicate that the Valanginian and Hauterivian intervals show a progressive decrease in reworked palynomorphs, culminating in almost a total lack of reworking during post-Hauterivian (Barremian-Aptian) deposition.

Modern Arctic Process Analogs

Modern processes that produce and distribute sediment in a seasonally cold marine setting at high latitude where glaciers are absent (for example, Lisitzin, 2002) form the basis of our interpretation of the studied Lower Cretaceous sections. In our study of the Mikkelsen Bay State 1 well cores, we commonly observed isolated, outsized mud-supported clasts, as well as crude lamination and pelleting, but very few other sedimentary structures were observed except for partial bioturbation and remnant upward fining laminae (Keller and Macquaker, 2001; Keller and others, 2001; Macquaker and Keller, 2005). Because of these features, we proposed that the melting of sediment-laden sea ice, analogous to modern forms of sea ice in the Beaufort Sea (Barnes and others, 1982; Kempema and others, 1989; Reimnitz and others, 1993; 1998), was an important source and transport mechanism of fine-grained sediment, as well as for some coarser grained sediment. Although rafting by ice or other means had been previously proposed to explain the presence of rare to common, mud-supported, outsized coarse grains, pebbles, and cobbles in the pebble shale unit (Bird and Molenaar, 1987; Molenaar, 1988), the mud, silt, and organic enrichment in this unit had not been previously attributed to rafting-related processes. However, studies in the modern Beaufort Sea by Kempema and others (1989) have shown that these finer sediment fractions are actually the most abundant ice-rafted sediment present.

It is worth noting that the abundance of the smaller size fractions in the modern Beaufort Sea—where silt is the average sediment size (Kempema and others, 1989)—is attributed to the pervasive presence of permafrost on the North Slope today, and in particular, to physical weathering by continual freezing and thawing which ultimately crushes all rock material to silt size (Lisitzin, 2002, p. 31). The regional permafrost on the North Slope results from several factors that produce a very cold semiarid to arid climate and a "humidity deficit" with respect to the amount of precipitation needed to form glaciers (Lisitzin, 2002). Therefore, large glaciers are absent in this part of the modern Arctic. The sediment delivered to the Beaufort Sea by fluvial systems on the North Slope consists of a large fine-grained fraction. Commonly, only minor coarser sediment is available to supply the sediment-laden, seasonal sea ice that forms there. We suggest that similar conditions may have prevailed during the Early Cretaceous deposition of the pebble shale unit and the lower part of the Hue Shale in this region, as evidenced by the predominance of fine-grained siliciclastic sediment and the absence of abundant poorly sorted and coarse-grained angular clasts, particularly striated coarser clasts (for example, Gilbert, 1990).

The formation of sea ice—primarily in the fall and sometimes during winter—also creates heavy brines that sink and disturb the water column (Anderson and Dyrssen, 1989; Reimnitz and others, 1998), sometimes eroding and resuspending sediment and at least episodically supplying more oxygen. This is consistent with observed bioturbation and agglutinated, benthic foraminifers within these Lower Cretaceous mudstones. Primary producers living mainly at the base of recent sea ice contribute a significant organic component (Horner, 1989), which is then pelletized by associated zooplankton. In the sea ice sampled from the modern Beaufort Sea, for example, approximately 30 percent of the sediment is pelleted (Reimnitz and others, 1993). More than 300 species belonging to 75 genera of microalgae, primarily diatoms, have been reported from Arctic sea ice (Horner, 1989, p. 126). During the following spring/summer when sea ice melts, the sediment in the ice subsequently settles from suspension directly below wherever the ice is at that time. In addition to algae within and associated with sea ice, a new and unexpected discovery of massive phytoplankton blooms under first-year sea ice by Arrigo and others (2012) shows that nutrient sources and conditions that enhance productivity in the Arctic are not completely understood.

Organic Richness—Petroleum Source Rock Potential

The need to better understand the petroleum source rock potential of the Lower Cretaceous mudstone succession of the North Slope both spatially and temporally was a major early objective of these studies (for example, Keller and others, 1999; 2001; Keller and Macquaker, 2001). Previous reports indicated different source-rock characteristics and quality for different parts of the North Slope—as different as the pebble shale being gas prone in the ANWR and oil prone at Prudhoe Bay (for example, Magoon and others, 1987). Results from high-resolution studies of the organic facies by Rock-Eval pyrolysis, biomarkers, and other geochemical methods for the Mikkelsen 1 well (Keller and Macquaker, 2001; Keller and others, 2001) showed surprisingly good source-rock potential for both the pebble shale unit and Hue Shale and more temporal variation (see full report in Keller and others, 2001) than other studies had shown. These Rock-Eval results are summarized and averaged in table 1 for the Mikkelsen Bay State 1 well for comparison with Rock-Eval results (by others) for the Orion 1 well done on cuttings (DGSI, Inc., 1997). We note that significantly better potential in the Orion 1 well occurs higher in the Hue Shale over a 40-ft interval (6,860–6,900 ft) above our lithofacies samples (fig. 5). Here, average total organic carbon (TOC) is 4.0 weight percent, hydrogen index (HI) is 311, and S_2—the amount of hydrocarbons (HC) generated by pyrolysis (plus some bitumen)—which is a measure of remaining petroleum source potential) is 12.6 milligrams of hydrocarbon per gram of rock (mg HC/g rock)—very similar to results for the pebble shale unit of the Mikkelsen Bay State 1 well.

No analyses were done on the Canning River outcrop samples during these studies because they are thermally mature with respect to oil generation and severely fractured by permafrost (Macquaker and others, 1999). A prior study showed that the range of values for organic richness—approximately 2–6 weight percent TOC—determined for the pebble shale unit in the Canning River section (Steve Bergman, oral commun., 1998) is similar to that of the Mikkelsen well. Another recent study corroborates these results (van der Kolk, 2010).

Table 1. Comparison of Rock-Eval pyrolysis data for the Mikkelsen Bay State 1 and Orion 1 wells in Arctic Alaska.

[Results are reported as the average and range of values. Note that Mikkelsen well data are summarized from results for 36 individual core samples (see Keller and others, 2001, for full report). Orion well data are reported as 10-foot (ft) intervals from "cuttings" (DGSI, Inc., 1997). However, these intervals were continuously cored in the Orion well, so rather than actual cuttings, these analyses are likely to have been done on a composite sample made up of pieces of core where one piece of core was contributed per 1.0 ft and then composited over a 10.0 ft interval for each "cuttings" sample. GRZ, the contiguous lower part of the Hue Shale, also defined as the gamma-ray zone; TOC, total organic carbon; S_1, free hydrocarbons (HC) less than approximately C_{33} volatilized by isothermal pyrolysis, in milligrams of hydrocarbon per gram of rock (mg HC/g rock); S_2, HC cracked from kerogen (and residual bitumen) by programmed pyrolysis, in mg HC/g rock; S_3, carbon dioxide (CO_2) released from kerogen by programmed pyrolysis to 390 degrees Celsius (°C), in mg CO_2/g rock; T_{max}, temperature of maximum S_2 yield in degrees Celsius; HI, hydrogen index; OI, oxygen index; S_2/S_3, an indicator of kerogen type; PI, production index; S_1/TOC, An indicator of thermal maturity or oil staining in a source rock, in mg HC/g organic carbon (C_{org}); N, number of samples]

Unit	TOC	S_1	S_2	S_3	T_{max}	HI	OI	S_2/S_3	PI	S_1/TOC	N
Mikkelsen Bay State 1 Well CORE[1]											
GRZ and upper part of pebble shale unit, samples 32–47, depth interval 11,606–11,635 ft	3.5 (2.1–5.6)	1.9 (<1–3.2)	7.2 (1.9–16.1)	0.47 (0.32–1.01)	435 (430–439)	204 (59–397)	14 (6–32)	17 (1.8–44.6)	0.23 (0.11–0.4)	0.56 (0.27–0.97)	16
Lower part of pebble shale unit, samples 12–31, depth interval 11,637–11,662.5 ft	4.0 (2.8–5.9)	1.35 (0.82–2.46)	13.6 (8.24–26.42)	0.44 (0.27–0.69)	438 (435–441)	336 (278–449)	11.4 (7–22)	32.3 (15.8–60.0)	0.09 (0.05–0.16)	0.34 (0.22–0.54)	20
Orion 1 Well "Cuttings"[2]											
Orion 1 Well "Cuttings"2 Lower part of Hue Shale GRZ depth interval 6,940–7,000 ft	3.3 (3.1–3.5)	0.30 (0.22–0.36)	6.7 (5.8–8.9)	0.47 (0.34–0.57)	429 (427–430)	202 (176–254)	14.5 (10–17)	14.4 (11.9–17.6)	0.04 (0.03–0.05)	0.90 (0.69–1.07)	6
Pebble shale unit depth interval 7,000–7,020 ft	3.5 (3.5)	0.35 (0.32–0.35)	7.4 (7.2–7.7)	0.50 (0.37–0.63)	427 (427)	211 (204–219)	14.5 (11–18)	15.8 (12.3–19.4)	0.04 (0.04)	0.95 (0.91–0.99)	2

[1]Mikkelsen Bay Well data from Keller and others (2001).

[2]Orion well data from DGSI, Inc. (1997).

Depositional Model for the Lower Cretaceous Succession

It seems reasonable to propose that similar processes of productivity and settling from suspension during the melting of sometimes sediment-laden seasonal sea ice in the modern Arctic occurred during deposition of the pebble shale unit in an Early Cretaceous Arctic Sea. These processes resulted in mostly fine-grained sediment deposition as various types of marine particle aggregates ("marine snow" where particles are greater than or equal to 0.5 mm) with both organic and mineral constituents (Alldredge and Silver, 1988). Additionally, these sea ice related processes are important for explaining deposition of some of the abundant pelleted mud and probably most of the uncommon mud-supported, isolated, sand and granule to pebble sized clasts that are present throughout the pebble shale unit and less commonly in the Hue Shale (see also Macquaker and Keller, 2005). Although the influence of deposition from melting sea ice is documented in the samples we have collected, this doesn't establish the overall importance of its contribution to the sediment supply and transport. Nevertheless, we observe the influence of sea ice throughout the pebble shale unit and into the lower parts of the Hue Shale that we've studied, becoming less important higher in the Hue Shale. The coarser grained basal part of the pebble shale unit was more likely deposited from melting anchor ice, river ice, fast ice, and perhaps also by some of the other rafting methods proposed previously, such as being carried by tree roots and kelp (Blanchard and Tailleur, 1983; Bird and Molenaar, 1987).

The sharp, commonly wavy based, crude bedding and crude upward fining in poorly sorted, commonly discontinuous, more silt-rich basal lenses and lamina of some of the beds in the pebble shale unit are also likely to have originated from suspension settling from melting seasonal sea ice. Here, the sediment load from melting ice essentially dropped to the sea floor without additional reworking or sorting by currents. These units rarely show evidence of scour or erosion below their wavy lower contacts; however, the form of these contacts could result from either subsequent differential compaction around the coarser basal laminae and discontinuous lenses or from compaction in combination with either some relief or armoring, such as from microbial mat formation, present on the uppermost clay-rich or clay-dominated lamina of the bed below.

Fluvial sources ultimately supplied much of the sediment in the Lower Cretaceous succession to the Early Cretaceous Arctic sea, although evidence of a minor aeolian contribution exists in the form of rare, rounded and pitted quartz grains that may have been blown onto the ice. These were particularly observed in the Mikkelsen well section of this study, and have also been observed (Blanchard and Tailleur, 1983) and documented by others (for example, Mickey and others, 2006). The mud and minor sand fraction was then transported and redistributed by storms, tidal and other currents, and various density flow processes interacting with seasonal sea ice and intermittently with sediment-laden seasonal sea ice.

Storm deposits and deposition from turbidity/density flows occurred at least locally and episodically in the area of the Orion well during deposition of the Hue Shale as evidenced by (1) a massive, centimeter thick, well sorted sand layer on a scoured surface; (2) an interval of thin, planar-laminated, graded, silt-dominated mudstones, separated by clay-dominated laminae, overlying a scoured angular surface; and (3) multiple intervals of thin sand-bearing silt-rich and silt-dominated mudstones that form the basal laminae of distinctive millimeter-scale beds/couplets that fine upward to clay-dominated laminae (fig. 12). In the Orion well, the latter beds are rare in the pebble shale unit but common in certain intervals of the Hue Shale (fig. 12*C*, *F*). Some of these beds may have been deposited by waning-flow processes like those that formed the rare silty-based, fining upward beds/couplets present in the Hue Shale of the Mikkelsen well (fig. 8*D*, *E*). Also present in the pebble shale unit of the Orion well are rare bedforms with sharp, irregular contacts of erosional cut and fill structures infilled by crudely upward fining laminae (fig. 8*C*). These are similar to structures described by O'Brien (1996) and Schieber (1999) and were likely produced by higher energy events such as major storms or from hyperpycnal (bottom-flowing) currents.

Biological processes were also episodically important to the origin of this fine-grained succession because it is relatively starved of siliciclastic sediment (Macquaker and Keller, 2005). Nutrients released from melting, sediment-laden sea ice (Measures, 1999) probably fueled high primary organic productivity in the marginal ice zone, and organisms associated with the ice produced fecal pellets that comprise much of the sedimentary detritus settling to the sea floor as marine particle aggregates (Reimnitz and others, 1998; Macquaker and Keller, 2005; Macquaker and others, 2010). Marine particle aggregates have a faster settling rate than individual grains and thus a decreased residence time in the water column once melting occurs. Therefore, a faster settling rate along with cold water, which also aids preservation of organic material (Honjo and Roman, 1978), and high productivity led to the deposition, at least locally, of organic carbon-rich pelagic sediment with a pelleted fabric (Macquaker and Keller, 2005). A number of studies (for example, Kranck and Milligan, 1980; 1991; Kranck, 1984; Kranck and others, 1996a) have shown that fine-grained sediment is commonly deposited as mud flocs—aggregates of clay and silt—rather than individual particles that reach the sea floor. It seems reasonable to propose that these mud flocs and aggregates would also occur in colder seas at high latitudes associated with the organic productivity occurring there.

In addition to the sediment supplied by fluvial, aeolian, and biological processes and subsequently transported by sediment-laden seasonal sea ice, storms, and various current and flow processes, volcanic sources also provided sediment and contributed nutrients to fuel productivity in the studied sections (Keller and others, 2001; Macquaker and Keller, 2005). In some parts of the pebble shale unit in the Mikkelsen succession, intervals consisting almost entirely of pellets are associated with beds of thin pyritized ash fall deposits. This suggests that after the ash landed in the sea, increased organic productivity and fecal pellet production contributed significant material to the sea floor (figs. 9*D*, 11*D*). This association also occurs in both the Hue Shale and the pebble shale unit of the Orion well (fig. 11*B*–*C*). Because tuffs and bentonites, by definition, are more common and thicker in the Hue Shale than in the pebble shale unit (fig. 5), this association would be expected to occur more abundantly in the Hue Shale.

Also prominent in both the Hue Shale and pebble shale unit are authigenic forms of pyrite and carbonate. As discussed previously for the Canning River section (Macquaker and others, 1999) and the Mikkelsen Bay well (Keller and others, 2001; Macquaker and Keller, 2005), pyrite occurs in multiple forms and in a broad size range, including very small crystals or framboids, suggesting diagenetic formation in the sediment within the zone of methanogenesis rather than formation in the water column. Pyrite in the Orion well core is also present in these same forms.

Carbonate-cemented intervals and concretionary carbonate units (observed in outcrop, for example, fig. 2) are present in both formations at all three locations. They are particularly noticeable in the pebble shale unit of the Canning River succession where they form units as much as 1.5 m thick. In the Orion and Mikkelsen wells, the cemented intervals in the pebble shale unit (shown schematically in fig. 5) are much thinner than in the Canning River section. In both wells, we sampled only the lower part of the cored Hue Shale (fig. 5); however, we observed that the carbonate cemented intervals in the total Hue Shale core are more numerous and thicker than in the pebble shale unit. At all three localities, these cemented units are predominantly composed of microcrystalline carbonate that fills the majority of the uncompacted, intergranular pore spaces at these levels. The carbonates are probably mainly the products of anaerobic microbial metabolic processes (for example, Irwin and others, 1977; Raiswell, 1988; Macquaker and Gawthorpe, 1993; Macquaker and others, 1999), and their presence indicates significant breaks in sediment accumulation at these levels (Macquaker and others, 1999) because considerable time is required to transport the solutes to fill all the uncompacted pore space with cement. Typically, cementation due to breaks in sedimentation is best developed at stratal surfaces (for example, Macquaker and Jones, 2002), particularly in distal depositional environments or areas away from sediment supply where clastic sediment starvation occurred (Macquaker and others, 2007).

Given the thickness and number of carbonate cemented units in the pebble shale unit of the Canning River section, it would seem that this area of the depositional basin experienced the most prolonged and possibly the greatest number of breaks in siliciclastic sediment accumulation during deposition of the pebble shale unit. These same events resulting in breaks in sedimentation, which could be due to flooding and relatively high sea level, are presumed to be either recorded differently or by the thinner cemented intervals in the pebble shale unit of the Orion and Mikkelsen sections. This is consistent with the Canning River section's location farther south (figs. 3 and 4) and therefore farther down the path of sediment transport by mechanisms other than sea ice during deposition of the pebble shale unit. However, this does not explain the much thicker siliciclastic component of the pebble shale unit in this comparatively more distal location (see fig. 5). It is possible that some sources of sediment bypassed the more proximal Orion and Mikkelsen locations and accumulated in more distal settings or that sediment was eroded by advective currents once deposited there, or a combination of both. In the Orion section, evidence of cut and fill structures and scoured surfaces suggest that some sediment was eroded by storms and other current and flow processes; however, most of these features occur in the Hue Shale and are rare in the pebble shale unit. The section in the Mikkelsen well shows only rare evidence of scour or erosion, which is consistent with the interpretation of Noonan (1987) that block faulting related to rifting occurred in this region. Perhaps this area was in a structurally higher position where sediment other than from ice rafting and pelagic sources bypassed it most of the time, with the exception of finer grained sediment transported in plumes rather than along the bottom. These processes are also consistent with the thinner than usual (200–400 ft thick) pebble shale unit sections of both wells (see fig. 5).

Summary and Conclusions

We document and interpret the origin of previously unknown lithofacies and organic facies variability and sedimentary textures and fabrics at millimeter scale in thin sections from three widely spaced localities of the Lower Cretaceous mudstone succession on the North Slope, Arctic Alaska—exposures at the Canning River (Macquaker and others, 1999) and in the Mikkelsen 1 (Keller and others; 2001, Keller and Macquaker, 2001; Macquaker and Keller, 2005) and Orion 1 wells. Most of these facies and the scale of their variation are not evident from macroscopic observation and had not been described before our reports on these sections.

These Lower Cretaceous sections of the pebble shale unit and lower part of the Hue Shale consist primarily of clay-rich mudstones that are silt or sand-bearing and clay-dominated mudstones that exhibit mainly relict, 2–5 mm thick bedding, common but variable microbioturbation, rare macrobioturbation, common fabrics of pelleted clay and silt, and rare evidence of erosion or scour. We interpret the common to rare occurrence of distinctive, mud-supported, outsized clasts of fine sand- to pebble-size throughout the pebble shale unit and more rarely in the Hue Shale, plus the presence of poorly sorted, silt-rich basal laminae with crude upward fining from sharp and wavy nonerosive bases to result from intermittent deposition by suspension settling from melting sediment-laden seasonal sea ice and associated primary productivity. We further propose that this succession formed in a cold, high latitude setting similar to the modern Beaufort Sea margin of

Arctic Alaska, where large glaciers are absent and permafrost significantly affects the fluvial input to the region. The origin of silt-rich basal laminae with crude fining upward is more equivocal than that of the outsize clasts; these laminae may have formed by weak density currents.

Although evidence of a minor aeolian contribution exists in the form of rare, rounded, frosted, and pitted quartz grains that may have been blown onto the ice, fluvial sources ultimately supplied much of the sediment that was deposited in the Early Cretaceous Arctic sea. This mud and minor sand was then transported and redistributed by storms, tidal and other currents, and various density flow processes interacting with seasonal sea ice and intermittently with sediment-laden seasonal sea ice. Storm deposits and deposition from turbidity/density flows occurred at least locally and episodically in the area of the Orion well during deposition of the Hue Shale.

The Lower Cretaceous sections generally fine and deepen (Mickey and others, 2006) upward into the Hue Shale from a coarser basal unit of pebbly to sandy mudstone and muddy sandstone in the pebble shale unit. Other important lithofacies are graded tuffs/bentonites and tuffaceous/bentonitic mudstones, which are abundant in the Hue Shale and newly discovered in rare intervals of the pebble shale unit of the Mikkelsen and Orion wells. Authigenic pyrite and carbonate-cement-dominated mudstone are also present in both units of all three successions. These carbonate-cemented units indicate that prolonged breaks in sedimentation were common during deposition of the Hue Shale, and also the pebble shale unit, particularly in more clastic-starved or distal settings such as the Canning River.

High-resolution study of the organic material in the Mikkelsen well shows that both formations contain primarily Type II, oil prone kerogen but have important internal variation in Rock-Eval parameters, probably due in part to multiple and changing sources of sediment. Thin volcanic ashes and associated pelleted organic-carbon rich intervals exhibited some of the best petroleum source rock potential in the pebble shale unit of the Mikkelsen well.

For the pebble shale unit, sediment-laden seasonal sea ice played a major role in episodically contributing mud and organics in addition to coarser sediment fractions. Although fluvial input in the studied sections of the pebble shale unit may be less important than sea ice, we note a greater influence of fluvial input in the Orion section compared to the others. For the Hue Shale, distal fluvial and volcanic-ash sources appear to be greater than sea ice. Also, apparently more common are periods of sediment hiatus during which carbonate cementation occurred. A modern setting that we consider to be a reasonable analog for the Early Cretaceous Arctic during deposition of the pebble shale unit is the modern Beaufort Sea margin. This region has a relatively high sea level, rivers supplying seasonal discharge, a semiarid to arid cold climate, and consequent permafrost but no large glaciers.

This study of three Lower Cretaceous mudstone sections on the North Slope of Arctic Alaska has yielded surprising new results at a millimeter scale on the textural and facies variation observed in these rocks. The implications of these characteristics for the processes that formed these rocks require us to reconsider classic notions about how "black shales" form implicit in previous interpretations of these units. Our observations and proposed model for the processes that formed these mudstone sections provide a new understanding of this important petroleum source rock succession and new insights about the climate and possible processes operating during part of the Early Cretaceous in Arctic Alaska. We also note that our microscale lithofacies observations and interpretations seem relevant to explaining a regional feature of these rocks that was previously puzzling. In particular, the description of the pebble shale unit as a "thin uniform blanket of sediment" over such a large area seemed problematic from a process point of view until the role of sea-ice rafting was better understood in the modern Arctic and could be applied to the Early Cretaceous.

References Cited

Alldredge, A.L., and Silver, M.W., 1988, Characteristics, dynamics, and significance of marine snow: Progress in Oceanography, v. 20, p. 41–82.

Alldredge, A.L., Passow, U., and Logan, B.E., 1993. The abundance and significance of a class of large, transparent organic particles in the ocean: Deep-Sea Research I, v. 40, p. 1131–1140.

Anderson, L. and Dyrssen, D. 1989, Chemical Oceanography of the Arctic Ocean, in Herman, Y., ed., The Arctic seas climatology, oceanography, geology, and biology: New York, Van Nostrand Reinhold, p. 93–114.

Arrigo, K.R., Perovich, D.K., Pickart, R.S., Brown, Z.W., van Dijken, G.L., Lowry, K.E., Mills, M.M., Palmer, M.A., Balch, W.M., Bahr, F., Bates, N.R., Benitez-Nelson, C., Bowler, B., Brownlee, E., Ehn, J.K., Frey, K.E., Garley, R., Laney, S.R., Lubelczyk, L., Mathis, J., Matsuoka, A., Mitchell, B.G., Moore, G.W.K., Ortega-Retuerta, E., Pal, S., Polashenski, C.M., Reynolds, R.A., Schieber, B., Sosik, H.M., Stephens, M., Swift, J.H., 2012, Massive phytoplankton blooms under Arctic Sea ice: Science, v. 336, p. 1408.

Barnes, P.W., Reimnitz, E., and Fox, D., 1982, Ice rafting of fine-grained sediment, a sorting and transport mechanism, Beaufort Sea, Alaska: Journal of Sedimentary Petrology, v. 52 p. 493–502.

Bergman, S.C., Decker, J., and Talbot, J., 1995, Upper Cretaceous tephra deposits, Canning River area, north Alaska [abs.]: Geological Society of America, Cordilleran Section Meeting, May 24–26, 1995, Abstracts with Program, v. 27, no. 5, p. 5.

Bergman, S.C., 2006, North Alaska Upper Cretaceous tephra—Eurasian or North American source calderas [abs.]: Abstracts with Program, Cordilleran Section Geological Society of America/Pacific Section American Association of Petroleum Geologists/Western Region Society of Petroleum Engineers Meeting, April, 2006, v. 38, no. 5, p. 90–91.

Bird, K.J., 1999, Assessment overview, in ANWR assessment team, The oil and gas resource potential of the 1002 Area, Arctic National Wildlife Refuge, Alaska: U.S. Geological Survey, Open-File Report 98–34, p. AO1–AO56.

Bird, K.J., 2001, Alaska; a twenty-first-century petroleum province, in Downey, M.W., Threet, J.C., and Morgan, W.A., eds., Petroleum provinces of the twenty-first century: American Association of Petroleum Geologists Memoir 74, p. 137–165.

Bird, K.J., and Bader, J.W., 1987, Regional geologic setting and history of petroleum exploration, *in* Bird, K.J., and Magoon, L.B., eds., Petroleum geology of the northern part of the Arctic National Wildlife Refuge, northeastern Alaska: U.S. Geological Survey Bulletin 1778, p. 17–25.

Bird, K.J., and Houseknecht, D.W., 2005, Oil and gas assessment of central North Slope, Alaska 2005: U.S. Geological Survey Fact Sheet 2005–3043, 2 p., available at http://pubs.usgs.gov/fs/2005/3043/.

Bird, K.J., and Molenaar, C.M., 1987, Stratigraphy, in Bird, K.J., and Magoon, L.B., eds., Petroleum geology of the northern part of the Arctic National Wildlife Refuge, northeastern Alaska: U.S. Geological Survey Bulletin 1778, p. 37–59.

Blanchard, D.C., and Tailleur, I.L., 1983, Pebble shale (Early Cretaceous) depositional environments in National Petroleum Reserve in Alaska (NPRA) [abs.]: American Association of Petroleum Geologists Bulletin, v. 67, p. 424–425.

Bromley, R.G., 1996, Trace Fossils: Biology, Taphonomy and Applications. (2nd Edition): Chapman and Hall, London, 361 p.

Brosgé, W.P., and Tailleur, I.L., 1971, Northern Alaska petroleum province, in Cram, I.H., ed., Future petroleum provinces of the United States—Their geology and potential: American Association of Petroleum Geologists Bulletin Memoir 15, v. 1, p. 68–99.

Carman, G.J., and Hardwick, P., 1983, Geology and regional setting of Kuparuk Oil Field, Alaska: American Association of Petroleum Geologists Bulletin, v. 67, p. 1014–1031.

Collins, F.R., and Robinson, F.M., 1967, Subsurface stratigraphic, structural, and economic geology, northern Alaska (NPR-4 and adjacent areas): U.S. Geological Survey Inv. Naval Petroleum Reserve No. 4 and adjacent areas open-file report, 252 p.

DGSI, Inc., 1997, TOC/rock-eval data for the following North Slope wells—Exxon Company USA OCS Y-0804 (Orion #1), Husky Oil NPR Operations Kuyanak #1, Husky Oil Operations South Barrow #16, Husky Oil Operations West Dease #1 cuttings and U.S. Navy South Barrow #3: Alaska Division of Geological and Geophysical Surveys Geologic Materials Center Data Report 276, 5 p.

Domack, E.W., 1988, Biogenic facies in the Antarctic glacimarine environment—Basis for a Polar glacimarine summary: Palaeogeography, Palaeoclimatology and Palaeoecology, v. 63, p. 357–368.

Eyles, N., 1993, Earth's glacial record and its tectonic setting: Earth-Science Reviews, v. 35, p. 1–248.

Frakes, L.A., and Francis, J.E., 1988, A guide to Phanerozoic cold polar climates from high-latitude ice-rafting in the Cretaceous: Nature, v. 333, p. 547–549.

Gilbert, R., 1990, Rafting in glacimarine environments, in Dowdeswell, J.A., and Scourse, J.D., eds., Glacimarine environments processes and sediments: Geological Society Special Publication 53, p. 105–120.

Gorsline, D.S., Nava-Sanchez, E., and Murillo de Nava, J., 1996, A survey of occurrences of Holocene laminated sediments in California Borderland Basins: products of a variety of depositional processes, in Kemp, A.E.S., ed., Palaeoclimatology and palaeoceanography from laminated sediments: Geological Society Special Publication No. 116, p. 93–110.

Haga, H., and Mickey, M.B., 2002, Reworked palynomorph trends in late Jurassic to Neocomian strata of the Colville delta region, Alaska [abs.]: Pacific Section American Association of Petroleum Geologists and Western Region Society of Petroleum Engineers, Joint Technical Conference, Program and Abstracts, p. 78.

Harwood, G., 1988, Microscopical techniques—II, Principles of sedimentary petrography, *in* Tucker, M.E., ed.,Techniques in sedimentology: Blackwell Scientific Publications, p. 108-173.

Honjo, S., and Roman, M.R., 1978, Marine copepod fecal pellets—production, preservation and sedimentation: Journal of Marine Research, v. 36, p. 45–57.

Horner, R.A., 1989, Arctic sea-ice biota, in Herman, Y., ed., The Arctic Seas Climatology, Oceanography, Geology, and Biology: Van Nostrand Reinhold, New York, p. 123-146.

Huber, B.T., 1998, Tropical paradise at the Cretaceous poles?: Science, v. 282, no. 5397, p. 2199–2200.

Irwin, H., Curtis, C., and Coleman, M., 1977, Isotopic evidence for source of diagenetic carbonates formed during burial of organic-rich sediments: Nature, v. 269, p. 209–213.

Jones, D.L., and Grantz, A., 1964, Stratigraphic and structural significance of Cretaceous fossils from Tiglukpuk Formation, northern Alaska: American Association of Petroleum Geologists Bulletin, v. 48, p. 1462–1474.

Keller, M.A., Bird, K.J., and Evans, K.J., 1999, Petroleum source rock evaluation based on sonic and resistivity logs—Chapter SR (source rocks), *in* ANWR assessment team, The oil and gas resource potential of the 1002 Area, Arctic National Wildlife Refuge, Alaska: U.S. Geological Survey Open-File Report 98–34, p. SR1–SR62, CD-ROM.

Keller, M.A., and Macquaker, J.H.S., 2001, High resolution analysis of petroleum source potential and lithofacies of Lower Cretaceous mudstone core (pebble shale unit and ?GRZ of Hue Shale), Mikkelsen Bay State #1 Well, North Slope Alaska, in Houseknecht D., ed., NPRA Core workshop, petroleum plays and systems in the National Petroleum Reserve—Alaska: SEPM Core Workshop 21, p. 37–56.

Keller, M.A., 2006, The potential of high-resolution mudstone studies for remodeling models of the earth's depositional systems—A case study of Arctic Alaska's Lower Cretaceous succession: Joint Society of Economic Paleontologists and Mineralogists/Geological Society of London Research Conference on the Application of Earth System Modeling to Exploration, Snowbird, Utah, July 11–13, 2006, Abstracts and Program, p. 32–35.

Keller, M.A., Macquaker, J.H.S., and Lillis, P.J., 2001, A high resolution study of petroleum source rock variation, Lower Cretaceous (Hauterivian and Barremian) of Mikkelsen Bay, North Slope, Alaska: U.S. Geological Survey Open-File Report 01–480, 3 sheets, available at http://pubs.usgs.gov/of/2001/of01-480/.

Keller, M.A., Macquaker, J.H.S., and Lillis, P.J., 2009, Organic carbon-rich sedimentation in an Early Cretaceous Arctic sea—Nutrients supplied by sediment-laden seasonal sea-ice and volcanic ash: American Association of Petroleum Geologists, Annual Convention and Exhibition 7–10 June 2009, Abstracts Volume, v. 18, p. 113.

Kemp, A.E.S., 1996, Laminated sediments as palaeo-indicators, in Kemp, A.E.S., ed., Palaeoclimatology and palaeoceanography from laminated sediments: Geological Society Special Publication No. 116, p. vii–xii.

Kempema, E.W., Reimnitz, E., and Barnes, P.W., 1989, Sea-ice sediment entrainment and rafting in the Arctic: Journal of Sedimentary Petrology, v. 59, p. 308–317.

Kemper, E., 1987, Das klima der kreide-zeit: Geologisches Jahrbuch, Reihe A, v. 96, p. 5–185.

Kranck, K., 1984, Grain-size characteristics of turbidites: Geological Society of London Special Publications, v. 15, p. 83–92.

Kranck, K., and Milligan, T.G., 1980, Macroflocs—Production of marine snow in the laboratory: Marine Ecology—Progress Series, v. 3, p. 19–24.

Kranck, K. and Milligan, T.G., 1991, Grain size in oceanography, *in* Syvitski, J.P.M., ed., Theory, Methods and Applications of Particle Size Analysis: Cambridge University Press, New York, p. 332–345.

Kranck, K., Smith, P.C., and Milligan, T.G., 1996a, Grain-size characteristics of fine-grained un-flocculated sediments I—'One-round' distributions: Sedimentology, v. 43, p. 589–596.

Kranck, K., Smith, P.C., and Milligan, T.G., 1996b, Grain-size characteristics of fine-grained un-flocculated sediments II—'Multi-round' distributions: Sedimentology, v. 43, p. 597–606.

Lisitzin, A.P., 2002, Sea-ice and iceberg sedimentation in the Ocean: Berlin, Springer-Verlag, 563 p.

Lowe, D.R., and Guy, M., 2000, Slurry-flow deposits in the Britannia Formation (Lower Cretaceous), North Sea—A new perspective on the turbidity current and debris flow problem: Sedimentology, v. 47, p. 31–70.

Macquaker, J.H.S., 1994, A lithofacies study of the Peterborough Member, Oxford Clay Formation (Jurassic), U.K.—An example of sediment bypass in a mudstone succession: Journal of the Geological Society of London , v. 151, p. 161–172.

Macquaker, J.H.S., and Adams, A.E., 2003, Maximizing information from fine-grained sediments—An inclusive classification of mudstones: Journal of Sedimentary Research, v. 73, p. 735–744.

Macquaker, J.H.S., and Gawthorpe, R.L., 1993, Mudstone lithofacies in the Kimmeridge Clay Formation, Wessex Basin, southern England—Implications for the origin and controls of the distribution of mudstones: Journal of Sedimentary Petrology, v. 63, p. 1129–1143.

Macquaker, J.H.S., Gawthorpe, R.L., Taylor, K.G., and Oates, M.J., 1998, Heterogeneity, stacking patterns and sequence stratigraphic interpretation in distal mudstone successions—Examples from the Kimmeridge Clay Formation, U.K., *in* Schieber, J., Zimmerle, W., and Sethi, P., eds., Shales and mudstones: Stuttgart, Schweizerbart'sche Verlagsbuchhandlung, p. 163–186.

Macquaker, J.H.S., and Jones, C.R., 2002, A sequence-stratigraphic study of mudstone heterogeneity—A combined petrographic/wireline log investigation of Upper Jurassic mudstones from the North Sea (U.K.), in Lovell, M., and Parkinson, N., eds., Geological applications of well logs: American Association of Petroleum Geologists Methods in Exploration Series, no. 13, p.123–142.

Macquaker, J.H.S., and Keller, M.A., 2005, Mudstone sedimentation at high latitudes—Ice as a transport medium for mud and supplier of nutrients: Journal of Sedimentary Research, v. 75, p. 696–709.

Macquaker, J.H.S., Keller, M.A., and Davies, S.J., 2010, Algal blooms and "marine snow"—Mechanisms that enhance preservation of organic carbon in ancient fine-grained rocks: Journal of Sedimentary Research, v. 80, p. 934–942.

Macquaker, J.H.S., Keller, M.A., and Taylor, K.G., 1999, Sequence stratigraphic analysis of the lower part of the pebble shale unit, Canning River, northeastern Alaska, *in* ANWR assessment team, The oil and gas resource potential of the 1002 Area, Arctic National Wildlife Refuge, Alaska: U.S. Geological Survey Open-File Report 98–34, p. SS1–SS28.

Macquaker, J.H.S., and Taylor, K.G., 1996, A sequence stratigraphic interpretation of a mudstone-dominated succession—The Lower Jurassic Cleveland Ironstone Formation, U.K.: Journal of the Geological Society of London, v. 153, p. 759–770.

Macquaker, J.H.S., Taylor, K.G., and Gawthorpe, R.L., 2007, High-resolution facies analyses of mudstones—Implications for paleoenvironmental and sequence stratigraphic interpretations of offshore ancient mud-dominated successions: Journal of Sedimentary Research, v. 77, p. 324–339.

Magoon, L.B., Bird, K.J., Burruss, R.C, Hayba, D., Houseknecht, D.W., Keller, M.A., Lillis, P.L., and Rowan E.L., 1999, Evaluation of hydrocarbon charge and timing using the petroleum system, *in* ANWR assessment team, The oil and gas resource potential of the 1002 Area, Arctic National Wildlife Refuge, Alaska: U.S. Geological Survey Open-File Report 98–34, p. PS1–PS66.

Magoon, L.B., Woodward, P.V., Banet, A.C., Jr., Griscom, A.B., and Daws, T.A., 1987, Thermal maturity, richness, and type of organic matter of source rock units, *in* Bird, K.J., and Magoon, L.B., eds., Petroleum geology of the northern part of the Arctic National Wildlife Refuge, northeastern Alaska: U.S. Geological Survey Bulletin 1778, p. 127–179.

McCave, I.N., Hall, I.R., Antia, A.N., Chou, L., Dehairs, F., Lampitt, R.S., Thomsen, L., van Weering, T.C.E., and Wollast, R., 2001, Distribution, composition and flux of particulate material over the European margin at 47°–50°N: Deep Sea Research II, v. 48, p. 3107–3139.

Measures, C.I., 1999, The role of entrained sediments in sea-ice in the distribution of aluminum and iron in the surface waters of the Arctic Ocean: Marine Chemistry, v. 68, p. 59–70.

Mickey, M.B., Haga, H., and Bird, K.J., 2006, Micropaleontology of selected wells and seismic shot holes, northern Alaska: U.S. Geological Survey Open-File Report 2006–1055, CD-ROM. (Also available at http://pubs.usgs.gov/of/2006/1055/.)

Molenaar, C.M., 1983, Depositional relations of Cretaceous and Lower Tertiary rocks, northeastern Alaska: American Association of Petroleum Geologists Bulletin, v. 67, no. 7, p. 1066–1080.

Molenaar, C.M., 1988, Depositional history and seismic stratigraphy of Lower Cretaceous rocks in the National Petroleum Reserve in Alaska and adjacent areas, *in* Gryc, G., ed., Geology and exploration of the National Petroleum Reserve in Alaska, 1974 to 1982, U.S. Geological Survey Professional Paper 1399, p. 593–621.

Molenaar, C.M., Bird, K.J., and Kirk, A.B., 1987, Cretaceous and Tertiary stratigraphy of northeastern Alaska, *in* Tallieur, I., and Weimer, P., eds., Alaskan North Slope Geology: Society of Economic Paleontologists and Mineralogists, Pacific Section, book 50, v. 1, p. 513–528.

Mull, C.G., 1987, Kemik Sandstone, Arctic National Wildlife Refuge, northeastern Alaska, *in* Tailleur I., and Weimer P., eds., Alaskan North Slope Geology: Society of Economic Paleontologists and Mineralogists, Pacific Section, book 50, v. 1, p. 405–431.

Nelson, P.H., Kibler, J.E., and Giberson, C.P., 1999, Well data and well plots, chapter WL, *in* ANWR assessment team, The oil and gas resource potential of the 1002 Area, Arctic National Wildlife Refuge, Alaska: U.S. Geological Survey Open-File Report 98–34, 26 p.

Noonan, W.G., 1987, Post-Ellesmerian depositional sequences of the North Slope subsurface, *in* Tailleur, I., and Weimer, P., eds., Alaskan North Slope geology, volume 1: Society of Economic Paleontologists and Mineralogists, Pacific Section, book 50, p. 459–477.

O'Brien, N., 1996, Shale lamination and sedimentary processes, in Kemp, A.E., ed., Palaeoclimatology and Palaeoceanography from Laminated Sediments: Geological Society of London Special Publication, v. 116, p. 23–36.

Peters, K.E., Magoon, L.B., Bird, K.J., Valin, Z.C., and Keller, M.A., 2006, North Slope, Alaska: Source rock distribution, richness, thermal maturity, and petroleum charge: American Association of Petroleum Geologists Bulletin, v. 90, p. 261-292.

Pike, J., and Kemp, A.E.S., 1996, Silt aggregates in laminated marine sediment produced by agglutinated foraminifera: Journal of Sedimentary Research, v. 66, p. 625-631.

Price, G.D., and Mutterlose, J., 2004, Isotopic signals from late Jurassic—early Cretaceous (Volgian–Valanginian) sub-Arctic belemnites, Yatria River, Western Siberia: Journal of the Geological Society, London, v. 161, p. 959–968.

Raiswell, R., 1988, Chemical model for the origin of minor limestone-shale cycles by anaerobic methane oxidation: Geology, v. 16, p. 641–644.

Reimnitz, E., McCormick, M., McDougall, K., and Brouwers, E., 1993, Sediment export by ice rafting from a coastal polynya, Arctic Alaska, U.S.A.: Arctic and Alpine Research, v. 25, no. 2, p. 83–98.

Reimnitz, E., McCormick, M., Bischof, J. and Darby, D.A., 1998, Comparing sea-ice sediment load with Beaufort Sea Shelf deposits—Is entrainment selective?: Journal of Sedimentary Research, v. 68, p. 777–787.

Schieber, J., 1994a, Evidence for episodic high-energy events and shallow water deposition in the Chattanooga Shale, Devonian, central Tennessee, U.S.A.: Sedimentary Geology, v. 93, p. 193–208.

Schieber, J., 1994b, Reflection of deep vs shallow water deposition by small scale sedimentary features and microfabrics of the Chattanooga Shale in Tennessee, *in* Embry, A.F., Beauchamp, B., and Glass, D.J., eds., Pangea—Global environments and resources: Canadian Society of Petroleum Geologists Memoir 17, p. 773–784.

Schieber, J., 1999, Distribution and deposition of mudstone facies in the Upper Devonian Sonyea Group of New York: Journal of Sedimentary Research, v. 69, p. 909–925.

Scotese, C.R., Nokleberg, W.J., Monger, J.W.H., Norton, I.O., Parfenov. L.M., Bundtzen, T.K., Dawson, K.M., Eremin, Frolov, Y.F., Fujita, Kazuya, R.A., Goryachev, N.A., Khanchuk, A.I., Pozdeev, A.I., Ratkin, V.V., Rodionov, S.M., Rozenblum, I.S., Shpikerman, V.I., Sidorov, A.A., and Stone, D.B., 2001, *in* Nokleberg, W.J., and Diggles, M.F., eds., Dynamic computer model for the metallogenesis and tectonics of the Circum-North Pacific: U.S. Geological Survey, Open-File Report 01–261, CD-ROM.

Spicer, R.A., 2002, Changing climate and biota, in Skelton, P., ed., The Cretaceous world: Open University, Cambridge University Press, p. 85–162.

van der Kolk, D.A., 2010, Geochemistry, sedimentology, and stratigraphy of the Lower Cretaceous pebble shale unit, northeastern Alaska: University of Alaska, Fairbanks, Masters thesis, 116 p.

van der Kolk, D.A., Newberry, R.J., Whalen, M.T., and Wartes, M.A., 2007, A characterization of the pebble shale unit and lower Hue Shale within the northeast Brooks Range, Alaska—What's with the high-radioactive zone? [abs.]: The Alaska Geological Society 2007 Technical Conference, Abstracts Volume, p. 29.

Walker, J.D., and Geissman, J.W., 2009, Geologic time scale version 4.0: Geological Society of America, 1 p., accessed January 31, 2013, at http://www.geosociety.org/science/timescale/.

Zakharov, V.A., 1994, Climatic fluctuations and other events in the Mesozoic of the Siberian Arctic, *in* Thurston, D.K., and Fujita, K., eds., Proceedings of the 1992 International Conference on Arctic Margins: United States Mineral Management Service Report 94–0040, p. 23–28.

Menlo Park Publishing Service Center, California
Manuscript approval date June 22, 2015
Edited by James W. Hendley II
Design and layout by Vivian Nguyen

Keller and Macquaker—**Arctic Alaska's Lower Cretaceous (Hauterivian and Barremian) Mudstone Succession**—Professional Paper 1814–B

ISSN 2330-7102 (online)
http://dx.doi.org/10.3133/pp1814B